Contract No:

This document was prepared in conjunction with work accomplished under Contract No. DE-AC09-08SR22470 with the U.S. Department of Energy (DOE) Office of Environmental Management (EM).

Disclaimer:

We put science to work.™

Savannah River National Laboratory™

OPERATED BY SAVANNAH RIVER NUCLEAR SOLUTIONS

A U.S. DEPARTMENT OF ENERGY NATIONAL LABORATORY • SAVANNAH RIVER SITE • AIKEN, SC

Examining the Role of Canister Cooling Conditions on the Formation of Nepheline from Nuclear Waste Glasses

J. H. Christian

September 2015

SRNL-STI-2015-00429, Revision 0

SRNL.DOE.GOV

DISCLAIMER

Printed in the United States of America

Prepared for
U.S. Department of Energy

SRNL-STI-2015-00429
Revision 0

Keywords: *nepheline, canister centerline cooled, waste canister, high level waste, vitrification, crystallization, differential thermal analysis*

Retention: *Permanent*

Examining the Role of Canister Cooling Conditions on the Formation of Nepheline from Nuclear Waste Glasses

J. H. Christian

September 2015

Prepared for the U.S. Department of Energy under contract number DE-AC09-08SR22470.

Savannah River National Laboratory™
OPERATED BY SAVANNAH RIVER NUCLEAR SOLUTIONS

REVIEWS AND APPROVALS

AUTHORS:

_____
J. H. Christian, Process Technology Programs Date

TECHNICAL REVIEW:

_____
K. M. Fox, Hanford Mission Programs Date

APPROVAL:

_____
E. N. Hoffman, Manager Date
Process Engineering Technology Group

_____
C. C. Herman, Director, Hanford Support Missions Date

ACKNOWLEDGEMENTS

The author thanks Phyllis Workman for assistance with glass fabrication and Matt Kesterson for development of the thermal model. Jake Amoroso and Fabienne Johnson provided guidance on the experimental approach and data interpretation. David Missimer provided XRD analyses of the glasses. Jarrod Crum at Pacific Northwest National Laboratory provided suggested glass compositions for testing. Funding for this work by the U.S. Department of Energy Office of River Protection Waste Treatment & Immobilization Plant Project through Inter-Entity Work Order M0SRV00101 managed by Albert A. Kruger is gratefully acknowledged.

EXECUTIVE SUMMARY

Nepheline ($NaAlSiO_4$) crystals can form during slow cooling of high-level waste (HLW) glass after it has been poured into a waste canister. Formation of these crystals can adversely affect the chemical durability of the glass. The tendency for nepheline crystallization to form in a HLW glass increases with increasing concentrations of Al_2O_3 and Na_2O. Thus, the Defense Waste Processing Facility (DWPF) uses a "nepheline discriminator" (ND), which relates the concentrations of SiO_2, Na_2O, and Al_2O_3 to a critical value of : $\frac{SiO_2}{SiO_2+Na_2O+Al_2O_3} > 0.62$. This discriminator is included as a DWPF process control constraint, where nepheline is not predicted to form above the discriminator concentration. Importantly, the ND is a compositional constraint that was developed to be applied to a single kinetic state, the canister-centerline-cooled (CCC) state. To date, the majority of studies seeking refinement of ND have focused on compositional effects to identify potential conservatism in the current ND.

In this study we report on new efforts aimed at understanding the kinetic factors that drive nepheline formation in simulated nuclear waste glasses. Specifically, we evaluated heat transfer simulations, validated by a previous full scale test on an instrumented canister, that predict the time and temperature conditions of glass at many locations inside a waste canister during pouring and subsequent cooling. Several of the thermal conditions predicted by the simulations were experimentally applied to simulant waste-glass-filled crucibles in laboratory scale furnaces. Since only a small fraction of glass in a canister is anticipated to experience the conditions needed for nepheline crystallization, we expected that crystallization would decrease and eventually halt as glass cooled farther from the canister centerline since temperatures quickly fall below the glass transition temperature (T_g) near the canister wall. This approach to developing laboratory scale cooling profiles represents a change from the CCC heat treatments used for most baseline studies, which as stated above, form the basis for the kinetic state of the ND.

Motivated by the prospect of higher waste loadings, the goal of this research was to identify the time and temperature conditions within a waste canister that promote nepheline crystallization. The overarching goal of this work is to identify conservatism in the ND constraint, which may be restricting access to glass compositional space that would otherwise be acceptable.

To better understand nepheline behavior, five simulated HLW glasses (identified as NP-Fe-3, NP2-23, US-37, US-18 and A4) that fail the ND constraint, and are therefore likely to be susceptible to nepheline formation during the CCC, were subjected to the approximate thermal conditions experienced by HLW glass at the "1 in. offset from centerline" position of a stainless steel waste canister. Powder X-ray Diffraction (XRD) showed that the glasses were crystal-free prior to heat treatment, but each was found to contain varying amounts of nepheline as the primary crystalline phase following the 1in. offset heat treatment.

Glasses NP-Fe-3 and US-18 were also subjected to the approximate thermal conditions experienced at the "6 in. offset from centerline" position of a waste canister. The temperatures experienced at this position in a waste canister are lower than those at the 1 in. offset position. XRD analysis again showed nepheline as the primary crystalline phase, but the amount was reduced relative to that of the 1 in. offset position heat treatment. These results show that the thermal conditions away from the canister centerline are not as effective at fostering nepheline crystallization as the centerline conditions are. Therefore, the large volume of glass that cools away from the centerline may only form small or negligible amounts of nepheline during cooling.

In an effort to identify the specific portions of the employed heat treatments that induce nepheline crystallization, we selected composition NP2-23 to undergo cooling under the extremely slow (0.2 ℃/min) and extremely fast (2 ℃/min) conditions that are known to occur in various places within a canister as shown by the thermal simulation data. XRD analysis of these glasses showed the glass to be XRD amorphous when cooled between 1150 ℃ and 850 ℃ at both rates. However, nepheline was observed for glasses cooled between 1150 ℃ and 750 ℃, 1150 ℃ and 650 ℃ and 1150 ℃ and 550 ℃ under slow cooling conditions only, thus suggesting the 2 ℃/min cooling rate may be above the critical cooling rate for avoiding nepheline crystallization.

As a corollary and in an additional effort to become more focused on the exact time and temperature conditions that drive nepheline crystallization in NP2-23 glass, differential thermal analysis was measured. The thermograms consistently showed 3 exothermic peaks, believed to be associated with crystal phase formation. This data was used as a guide toward development of additional heat treatments for NP2-23. Using XRD, optical and scanning electron microscopy (OM and SEM respectively) the DTA data has been related to the crystallization events for glass composition NP2-23.

The results presented herein highlight the crucial role of time and temperature on nepheline formation, and show the kinetic conditions under which nepheline is prone to form in the studied glasses. As a path forward, it is recommended that computer simulations be performed to determine the exact volume of glass in a canister that cools under certain cooling rates. These simulations combined with the results herein could help to predict the total volume of nepheline present in a waste canister once it has cooled. Additionally, it is recommended that strategies be developed to increase the cooling rate of glass within a canister as this appears to be a crucial parameter affecting the amount of nepheline that forms during canister cooling.

TABLE OF CONTENTS

LIST OF TABLES

LIST OF FIGURES

LIST OF ABBREVIATIONS

CCC	Canister Centerline Cooling
DWPF	Defense Waste Processing Facility
DOE	Department of Energy
DSC	Differential Scanning Calorimetry
DTA	Differential Thermal Analysis
EDS	Energy Dispersive Spectroscopy
T_g	Glass Transition Temperature
HLW	High-Level Waste
T_L	Liquidus Temperature
ND	Nepheline Discriminator
NAS	Na_2O-Al_2O_3-SiO_2
OB	Optical Basicity
OM	Optical Microscopy
PCCS	Product Composition Control System
PCT	Product Consistency Test
SRNL	Savannah River National Laboratory
SRS	Savannah River Site
SEM	Scanning Electron Microscopy
TTT	Time-Temperature-Transformation
WTP	Waste Treatment Plant
XRD	X-ray Diffraction

1.0 Introduction

The structure of nepheline ($K/NaAlSiO_4$) is based on a tridymite-type framework containing 32 oxygen atoms per unit cell, in which approximately half of the silicon atoms are replaced by aluminum.[1] Nepheline can form during slow cooling of nuclear waste glass after it has been poured in a waste canister. Nepheline crystals can weaken the glass network from which they formed by depleting certain glass-formers in the matrix and creating grain boundaries which can preferentially leach. This occurs, because each mole of nepheline removes three moles of glass-forming oxides (Al_2O_3 and $2SiO_2$) per each mole of Na_2O or K_2O. Consequently, nepheline formation usually results in reduced chemical durability as measured by many durability tests in the 1980s[2] and 1990s[3]. Like all crystallization, nepheline formation depends on chemical, thermodynamic, and kinetic factors. Time-Temperature-Transformation (TTT) diagrams of nuclear waste glasses have shown that nepheline does not form above 750 ℃ in high SiO_2 glass, but in high alkali glass, it can form at higher temperatures.[2]

Currently a nepheline discriminator (Eq. 1) is used as a process control constraint at the DWPF.[4,5,6,7]The discriminator relates the concentrations of SiO_2, Na_2O, and Al_2O_3 (as weight fractions in glass) to a critical value of 0.62. If the discriminator ratio falls above 0.62, as is the case in glasses high in SiO_2, then no nepheline should form; however, glasses falling below 0.62 are considered prone to nepheline crystallization, upon slow cooling. This discriminator defines a boundary line on the Na_2O-Al_2O_3-SiO_2 (NAS) ternary diagram above which nepheline is not predicted to crystallize.

$$\frac{SiO_2}{SiO_2+Na_2O+Al_2O_3} > 0.62 \quad \textbf{(1)}$$

Although the nepheline discriminator imposes a useful restriction on glass compositions in order to avoid unwanted nepheline crystallization during slow cooling, it only considers the concentration of species within the NAS ternary despite the large compositional complexity of HLW glass. In recent years there have been efforts aimed at refining the nepheline discriminator in order to eliminate possible conservatism, which may be restricting access to glass composition regions that would otherwise be acceptable for processing.

Specifically, Fox[8] found a series of glass compositions that were very durable despite having nepheline discriminator values well below the limit of 0.62, but when this result was explored to identify linear effects of composition on nepheline crystallization the results were not sufficient to recommend modification of the nepheline discriminator.[9] Another effort by Fox[10] looked to develop an alternative nepheline discriminator model using theory of crystallization in mineral and glass melts, but again the results, in their current state, were unsuccessful in predicting nepheline crystallization in the studied glasses. McCloy et al. recently proposed that an additional constraint, optical basicity (OB), be used to complement the ND.[11] The OB constraint uses an electronegativity approach to rank constituent oxides according to their propensity to disassociate. This constraint was used to describe the effects of B_2O_3 and CaO on nepheline crystallization in HLW glasses, but again the results were not sufficient to recommend ND modification.

In 2011 Amoroso[12] took a non-compositional approach towards investigating possible ND refinement by evaluating the kinetics of nepheline formation for DWPF-related glasses. The results showed that the amount of nepheline ranged from approximately 2 wt.% to 30 wt.% depending on whether the samples cooled over short or long times. In some glasses nepheline crystallization appeared directly proportional to the total cooling time, but in other cases the crystallization appeared to be inversely proportional. These results highlighted the important role that kinetics play in nepheline formation and showed that refinement of the ND might be possible through additional kinetic studies.

Importantly, none of these studies differentiated the "type" of nepheline that formed since low temperature nepheline (hexagonal symmetry) can exist up to 875°C and then transforms to high temperature nepheline (orthorhombic). The ring structured aluminosilicate framework of nepheline forms cavities within the framework. There are eight large coordination sites that bond Ca, K, and Cs ionically to nine framework (Al,Si tetrahedral) oxygens and six smaller coordination sites that bond Na ionically to eight framework (Al,Si tetrahedral) oxygens.[13] The larger nine-fold sites can hold large cations such as Cs, K, and Ca while the smaller sites accommodate the Na. The K nepheline is known as kalsilite (KAlSiO4). A cubic sodium rich nepheline, $(Na_2O)_{0.33}NaAlSiO_4$[14], also exists and nephelines can be non-stoichiometric with varying substitution of Al and Si. In nature, the nepheline structure is known to accommodate Fe, Ti and Mg as well.[13]

To properly understand the kinetics of nepheline crystallization in a waste canister it is important to know the glass time and temperature conditions after it has been poured into a canister. Historically, studies of nepheline formation in HLW glass have utilized data from the centerline of full instrumented canisters to develop cooling profiles; however, as computational techniques become more commonplace, it is increasingly more convenient to use these tools to simulate the approximate thermal conditions inside of a waste canister.

In the study herein, simulated time and temperature conditions were replicated in laboratory scale crucibles in order to observe the role of kinetics in nepheline formation from nuclear waste glasses. Additionally, cooling under slow and fast conditions was employed in order to better focus on the specific time and temperature conditions that drive nepheline crystallization. Finally, Differential Thermal Analysis (DTA) was used to identify possible crystallization temperature ranges and the results were verified using 24 hr. heat treatments at various temperatures near where DTA exotherms were observed.

2.0 Experimental Procedure

2.1 Glass Composition Selection

Five glasses were selected for this study based on previous observations of being amorphous when quenched, but forming nepheline as the primary crystalline phase during CCC. The ND values for these glasses range from 0.48 – 0.60, thus each glass fails the discriminator to a varying degree as shown in Table 2-1 and Figure 2-1. Additionally, two of the glasses (US-18 and US-37) contain noble metals, which are known to be insoluble in the glass melt.[15]This provided an opportunity to study a fairly broad compositional region in order to evaluate the extent of nepheline formation under canister cooling conditions.

Table 2-1. The ND values and crystalline phases formed for the glasses in this study after both quenching and slow cooling.

Glass ID	Nepheline Discriminator	Previously Reported Phase After Quenching	Previously Reported Phase(s) After CCC
NP-Fe-3	0.53	Amorphous[16]	Nepheline Only[16]
NP2-23	0.60	Amorphous[9]	Nepheline Only[9]
US-18	0.59	Amorphous[17]	Nepheline Only[17]
US-37	0.56	Amorphous[17]	Nepheline and Iron Oxide[17]
A4	0.48	Amorphous[16]	Nepheline Only[16]

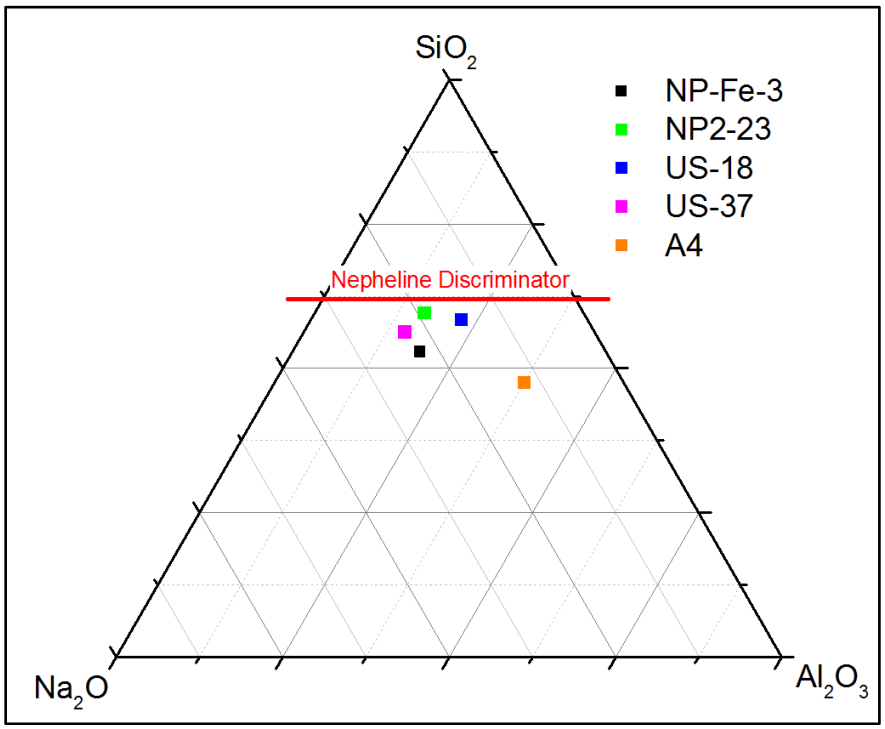

Figure 2-1. The location of the 5 studied glasses on the Na_2O-Al_2O_3 SiO_2 (NAS) ternary diagram along with the nepheline discriminator. The selected glasses cover a fairly broad range of ratios in these components.

Table 2-2. Targeted Compositions for Test Glasses in Weight Fraction. (The components of the ND are highlighted).

Glass Identifier	NP-Fe-3	NP2-23	US-18	US-37	A4
Al_2O_3	0.1331	0.1228	0.16	0.1	0.2402
BaO	0.0032	-	-	-	-
B_2O_3	0.0774	0.045	0.0913	0.0577	0.1199
CaO	0.0108	0.04	0.01	0.01	0.0608
CdO	0.0002	-	-	-	-
Cr_2O_3	0.0019	0.0002	-	-	0.0052
CuO	0.0003	-	-	-	-
Fe_2O_3	0.1295	0.0722	0.0975	0.17	0.0591
K_2O	0.001	-	-	-	0.0014
Li_2O	0.0435	0.04	0.0495	0.02	0.0677
MgO	0.0066	0.015	-	-	0.0012
MnO	0.0039	0.0119	0.03	-	-
Na_2O	0.1962	0.18	0.1341	0.1889	0.0959
NiO	0.0007	0.0017	-	-	0.004
P_2O_5	0.0094	-	-	-	0.0105
PbO	0.0026	-	0.001	0.01	0.0041
RuO_2	-	-	0.0002	0.0002	-
Sb_2O_3	0.0015	-	-	-	-
SO_3	-	-	-	-	0.002
SiO_2	0.3714	0.4494	0.4145	0.3733	0.3051
SrO	0.0001	-	0.001	-	-
TiO_2	0.0016	0.02	0.01	0.01	-
ZnO	0.0001	-	0.001	0.02	0.0008
ZrO_2	0.0028	-	-	0.04	0.004

2.2 Glass Fabrication

Each of the studied glasses was prepared from the proper proportions of reagent-grade metal oxides, carbonates, boric acid, and salts in 300 g batches. The raw materials were mixed and placed into 250 mL platinum/gold crucibles. Lids were placed on top of the crucibles to prevent contamination from furnace refractory and dust particles. Batches were placed into a high-temperature furnace at the targeted melt temperature of 1150 ℃. The crucibles were removed from the furnace after an isothermal hold at the melt temperature for 1 hour. The glass was poured onto a clean, stainless steel plate and allowed to air cool (quench). The quenched glass pour patties were evaluated using X-ray Diffraction (XRD) to confirm an amorphous glass structure. These glasses were used as the stock for all kinetic studies described herein.

2.3 Computer Simulations

Simulations of the thermal conditions present in a Waste Treatment Plant (WTP) HLW canister, employing a 29 min pour time with a 58 min pause between pours, were performed by Kesterson[18] using finite element modeling computer software. The stainless steel canister used for simulations is depicted in Figure 2-2. The colored circles in this figure represent the many areas within the canister where the temperature was simulated. The green circles are positioned 1” offset from the canister centerline where glass is poured. The yellow and blue circles are 6” and 12” offset from the centerline, respectively. The horizontal red lines mark the tops and bottoms of glass pours. At each canister position the temperature is simulated directly in the middle of a pour, at 0.25” above the bottom of a pour, and at 0.25” below the top of a pour. The bold numbers **1** and **2** label the canister positions where the thermal conditions were experimentally employed on the glasses in this study (see below).

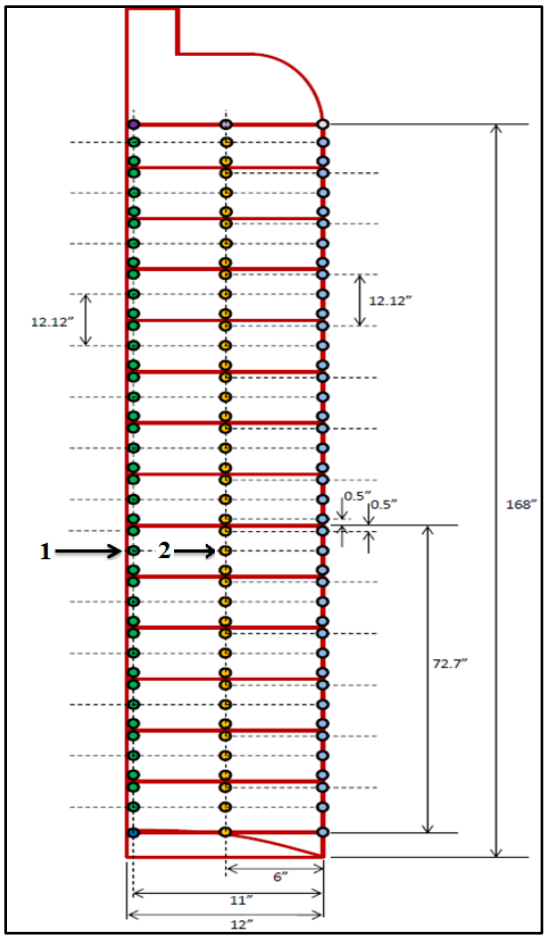

Figure 2-2. Cross-section of half of the HLW canister used for thermal simulations.

2.4 Simulated Canister Thermal Conditions

Simulated canister thermal conditions were used to develop lab-scale heat treatments for the 5 glasses. The time and temperature conditions along the centerline of a HLW canister (1" offset from direct center) at the midpoint of a glass pour are shown in Figure 2-3. The simulated temperature probes register their maximum temperature (T_{max}) at the moment they become covered with glass, thus the points prior to T_{max} simply represent heating of the air around the probes as glass fills the canister from the bottom up. These thermal conditions are of no concern when designing lab-scale heat treatments, since the glass itself will not experience these temperatures. It is therefore more convenient to view the simulated conditions starting at T_{max} (i.e., when the glass reaches the temperature probe). Removing the temperature profile of each probe prior to the time that it is covered with glass and superimposing the profiles so they all start at time = 0 yields Figure 2-4.

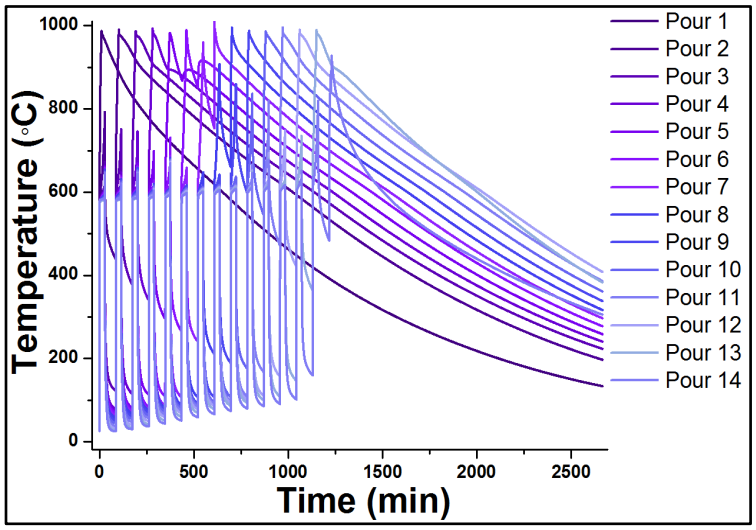

Figure 2-3. Simulated time and temperature conditions at the 1" offset from canister centerline position and at the midpoint of a glass pour.

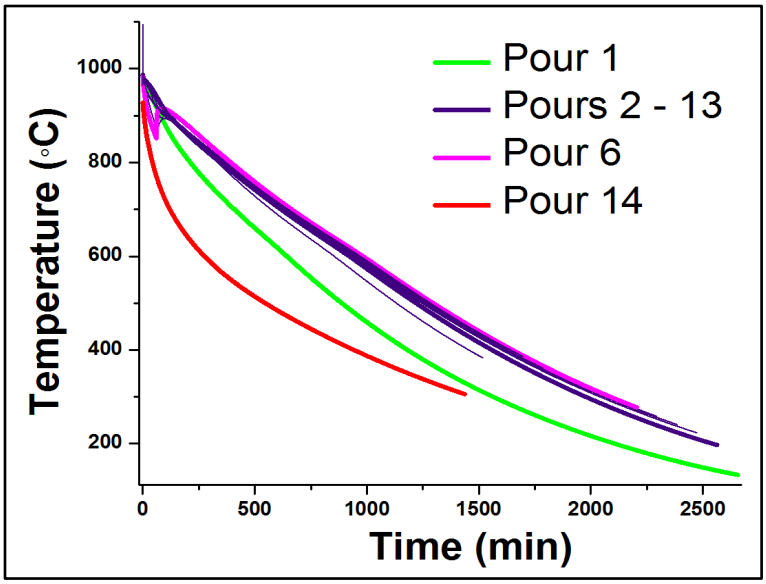

Figure 2-4. Simulated time and temperature conditions at the 1" offset from canister centerline position and at the midpoint of a glass pour. The profiles start at the time when the glass reaches the temperature probes.

Superimposition of the curves shows that the thermal conditions for each temperature probe are essentially the same except for the first and fourteenth (final) pour. This result significantly reduces the number of unique heat-treatments needed to evaluate the kinetics of nepheline formation.

As glass flows further from the canister centerline, temperatures are reduced and cooling rates are increased. The time and temperature conditions at 6 in. and 12 in. offsets from the canister centerline at the midpoint of a glass pour are shown in Figure 2-5. Importantly, by the time glass reaches the canister wall it is estimated to be near or below T_g[19], thus the formation of crystalline phases should be negligible. These data suggest that nepheline is most likely to form near the center of the canister, and that the propensity for crystallization should be reduced as glass flows further from the canister centerline.

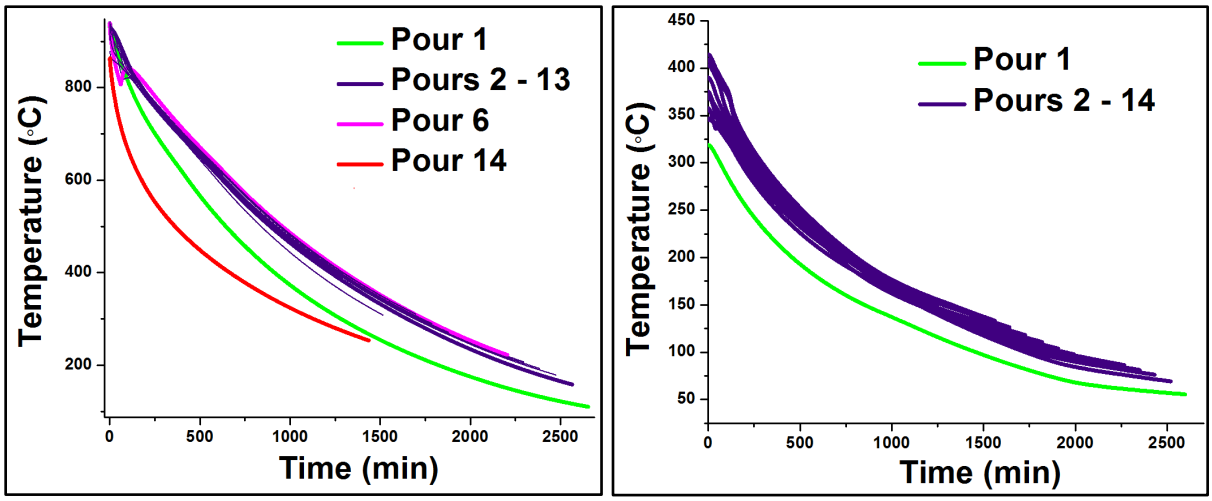

Figure 2-5. Simulated temperature profiles at the midpoint of a pour and 6" (left) and 12" (right) offset from the canister centerline. The data starts at T_{max} and is normalized so the pour conditions are superimposed.

For comparison, in Figure 2-6 the WTP HLW CCC time and temperature conditions are shown along with the thermal simulations of pour 6 from Figure 2-4 and Figure 2-5.When compared side-by-side it is clear that the thermal history of glass subjected to the CCC heat treatment (where glass is continuously poured) is noticeably different than the simulated history where glass is poured in discrete batches and is cooled away from the canister centerline. Specifically, glass is cooled from 1050 ℃ to 500 ℃ in approximately 1447 min in the CCC, 1315 min in the 1 in. offset simulation and 972 min in the 6 in. offset simulation. By the time glass reaches the 12 in. offset position the temperature is approximately 415 ℃ .

An important goal of the studies presented herein was to determine how these different thermal histories have an effect on the amount of nepheline that forms during cooling. All of the glasses studied in this report were exposed to the cooling profile of pour 6 in Figure 2-6. NP-Fe-3 and US-18 were also exposed to the cooling profile of pour 6 in Figure 2-5 (left). Furnace set temperatures, dwell times, and ramp rates of these profiles are listed in Table 2-3.

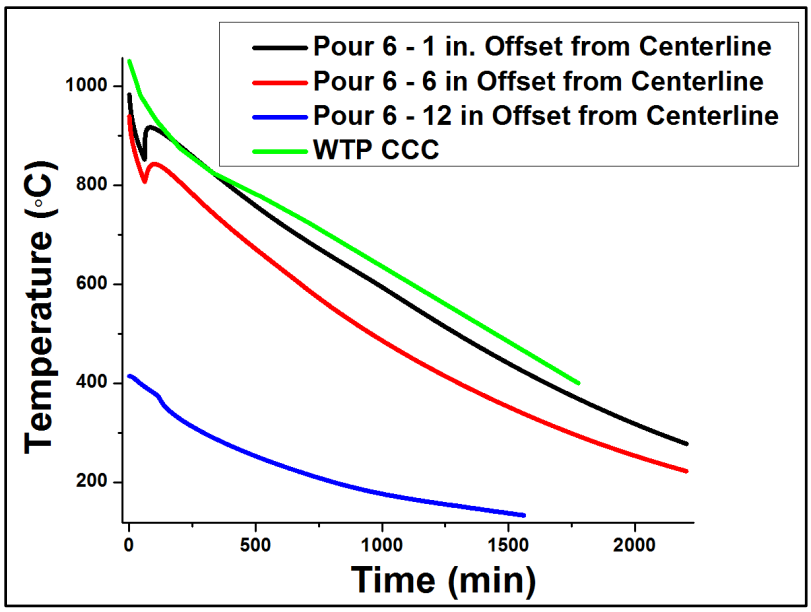

Figure 2-6. The simulated pour 6 temperature profiles are plotted with the WTP CCC cooling profile.

Table 2-3. Target setpoint and cooling rates used to replicate the thermal conditions at points 1 and 2 in Figure 2-2.

Heat Treatment 1	Start Setpoint (°C)	End Setpoint (°C)	Rate (°C/min)	Heat Treatment 2	Start Setpoint (°C)	End Setpoint (°C)	Rate (°C/min)
	1150	1150	Isothermal for 60 min.		1150	1150	Isothermal for 60 min.
	1150	986	25.00		1150	943	25.00
	986	920	4.12		943	888	4.44
	920	853	1.52		888	807	1.68
	853	920	2.64		807	843	1.26
	920	885	0.34		843	843	Isothermal for 28 min.
	885	755	0.40		843	591	0.43
	755	595	0.34		591	457	0.34
	595	395	0.29		457	344	0.26
	395	265	0.23		344	275	0.21
	265	0	∞		275	0	∞

As can be seen in Figure 2-7, when the heat treatments in Table 2-3 are plotted with the canister simulations they were designed to mimic, there is an excellent match between the two.

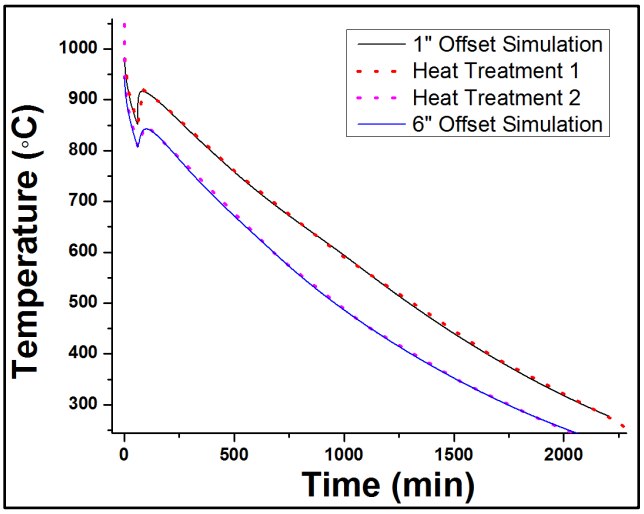

Figure 2-7. Heat Treatments 1 and 2 (dashed lines) are shown with the canister simulation data for the middle of a pour, 1" and 6" offset from the canister centerline position.

The thermal simulation data were analyzed to find the fastest and slowest cooling rates present amongst the entire canister dataset. The data showed that the fastest cooling rate, excluding the initial sharp drop after glass leaves the melter, is approximately 2 ℃/min. The slowest cooling rate is approximately 0.2 ℃/min. These cooling rates are plotted alongside the entire canister simulation dataset in Figure 2-8. To evaluate the effects of specific time and temperature regions on glass transformation, NP2-23 was subjected to cooling between 1150 ℃ - 950 ℃, 1150 ℃ - 850 ℃, 1150 ℃ - 750 ℃, 1150 ℃ - 650 ℃, and 1150 ℃ - 550 ℃ at cooling rates of 2 ℃/min and 0.2 ℃/min. The glass was rapidly quenched after reaching the end temperature and samples were analyzed via XRD.

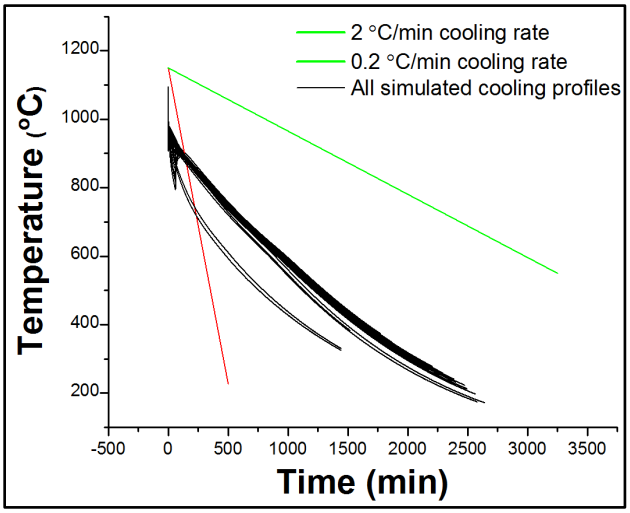

Figure 2-8. The full thermal simulation dataset is shown with lines representing roughly the fastest (2°C/min) and slowest (0.2°C/min) cooling rates seen in the simulations.

2.5 Validating Simulated Canister Thermal Conditions

Before applying the heat treatments in Table 2-3 to the simulated waste glass, the time and temperature conditions experienced by glass in a programmable furnace were first verified. Since the thermal conductivity of glass is significantly different than the thermal conductivity of air inside of the furnace we wanted to ensure the programmed furnace temperature matched the internal glass temperature. To perform this validation, a 30 g piece of crushed waste glass simulant in a 40 mL Pt/Au crucible was melted several times. A type-K thermocouple was securely positioned at the center of the glass shards before they were melted. The glass was then subjected to one of the heat treatments in Table 2-3. The temperature of the thermocouple was logged every 10 seconds, and was later analyzed to determine how well the actual thermal conditions matched the intended cooling profile.

2.6 Property Measurements

2.6.1 X-ray Diffraction

Quenched and heat treated samples were measured using XRD to identify and quantify any crystallization. Samples were carefully sectioned from a glass puck using a low speed saw. The samples were cut in a manner to include air and crucible interfaces and bulk glass. Samples were ground in an automatic Spex mill for 4 minutes. Subsequently, the powders were hand ground in agate with alcohol and mounted to a glass slide using a collidion/Amyl Acetate solution for XRD. The measurement conditions provided a 0.5 wt.% detection limit. If a broad hump(s) was measured then the sample was considered X-ray amorphous under the measurement conditions.

2.6.2 Scanning Electron Microscopy

Scanning Electron Microscopy (SEM) and Energy Dispersive Spectroscopy (EDS) measurements were performed with a Hitachi TM3000 SEM. EDS mapping of Na, Mg, Al, Si, Ca, Ti, Cr, Mn, Fe, and Ni was performed to identify crystalline phases formed during heat treatment.

2.6.3 Optical Microscopy

An Olympus SZX16 optical microscope with an image acquisition system was used to define the presence and approximate size of crystals in heat treated glasses.

2.6.4 Differential Thermal Analysis

Thermal analysis was performed using a Netzsch STA 409 PC TGA/DTA. The measurements were carried out in platinum pans in N_2 atmosphere (40 mL/min) with a 5 ℃/min heating rate. The crystallization temperature was taken at the maximum of exothermic peaks.

3.0 Results and Discussion

3.1 Temperature Profile Validation

The internal glass temperature, measured using a type-K thermocouple placed at the center of the glass before it was melted, showed that the temperature consistently matched the prescribed heat treatment within ± 20 ℃. The deviation is likely due to thermal gradients present within the glass and the thermocouple resting at slightly different positions during each measurement.

3.2 Heat Treating Waste Glass Simulants

The crystalline phase(s) identified and quantified for each waste glass simulant following heat treatment are given in Table 3-1.

Table 3-1. Quantitative XRD Results for Heat Treated Glasses

Glass ID	Phase After Quenching	Phases(s) After Heat Treatment 1	Previously Reported Phase(s) After CCC	Phase(s) After Heat Treatment 2
NP-Fe-3	Amorphous	Nepheline : 24.0 wt. %	Nepheline: 31.5 wt. % [16]	Nepheline : 14.1 wt. %
US-18	Amorphous	Nepheline : 5.7 wt. %	Nepheline: 4.7 wt. % [17]	Nepheline : 1.4 wt. %
US-37	Amorphous	Nepheline : 12.9 wt. % Trevorite : 2.8 wt. %	Nepheline: 12.5 wt. % Trevorite: 0.78 wt. % [17]	Not measured
A4	Amorphous	Nepheline : 16.0 wt. % Trevorite : 3.5 wt. %	Nepheline: 20.8 wt. % [16]	
NP2-23	Amorphous	Nepheline :6.4 wt. %	Nepheline : 5.6 wt. % [9]	

The amount of nepheline measured in each glass after heat treatment 1 is close to the amount previously reported after CCC. Specifically, when comparing the heat treatment 1 results to previously reported CCC results, NP-Fe-3 saw a 7.5 wt. % nepheline decrease, US-18 saw a 1.0 wt. % increase, US-37 saw a 0.4 wt. % nepheline increase, A4 saw a 4.8 wt. % nepheline decrease, and NP2-23 saw a 0.8 wt. % nepheline increase. The slight change in amount of nepheline may be due to different sampling procedures, use of different XRD quantitative calibration methods, but may also highlight how kinetics and the application of different cooling profiles can affect the degree of nepheline formation. Nonetheless, the WTP CCC appears to provide a fine representation of the canister conditions of heat treatment 1.

When NP-Fe-3 and US-18 were subjected to heat treatment 2, the glasses showed a 9.9 wt. % and 4.3 wt. % reduction in nepheline respectively compared to their heat treatment 1 counterparts, and a 17.4 wt. % and 3.3 wt. % decrease compared to their CCC counterparts. These results are in agreement with the postulate that the time and temperature conditions in a waste canister become less fostering of nepheline crystallization the farther the glass cools from the canister centerline. As stated in Section 2.4, glass is cooled from 1050 ℃ to 500 ℃ in approximately 1,447 min in the CCC, 1,315 min in the 1 in. offset simulation, and 972 min in the 6 in. offset simulation. Thus, the difference in these cooling rates contributes noticeably to the amount of nepheline formed.

Photos of the heat treated glasses are shown in Figure 3-1 and Figure 3-2. Each glass with the exception of NP2-23 shows obvious crystallization following heat treatment, although the nature of the crystallization appears different in most glasses. For example, in NP-Fe-3 the crystallization seems to emanate from the glass interfaces while in US-18, US-37, and A4, the crystals appear somewhat evenly dispersed throughout the glass. This observation in US-18 and US-37 is likely due to the presence of insoluble RuO_2 nucleation sites. Additionally, while US-18 and US-37 show the presence of small spot-like crystals, A4 contains fairly large, well-defined crystals. When comparing NP-Fe-3 and US-18 after heat treatment 1 and 2**,** the amount of crystallization is noticeably diminished after **2**, a result that further suggests the time and temperature conditions of 1 are more fostering of nepheline than 2.

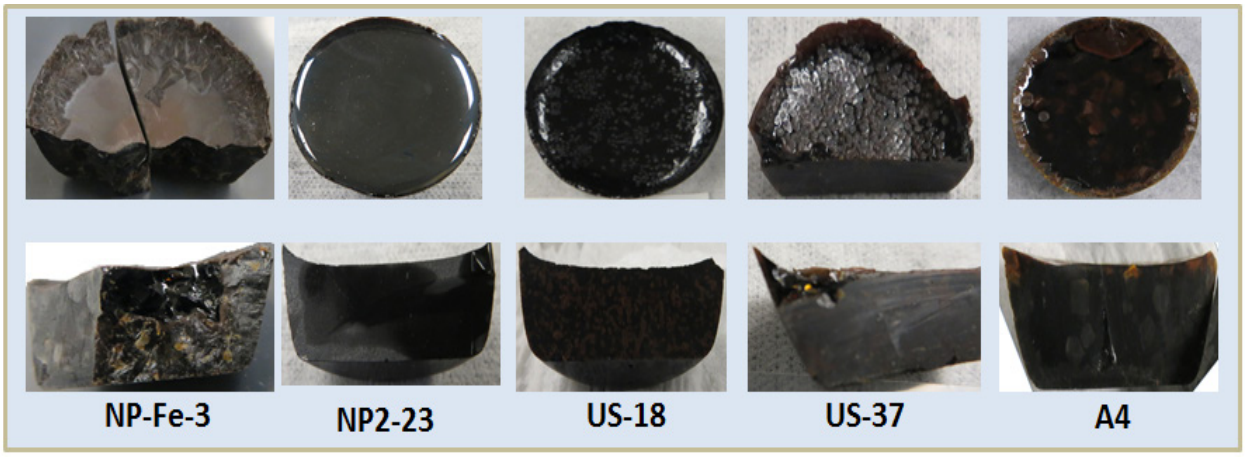

Figure 3-1. Photographs of glass subjected to heat treatment 1. Top: Glass-air interface. Bottom: Cross-sectional slice used for XRD.

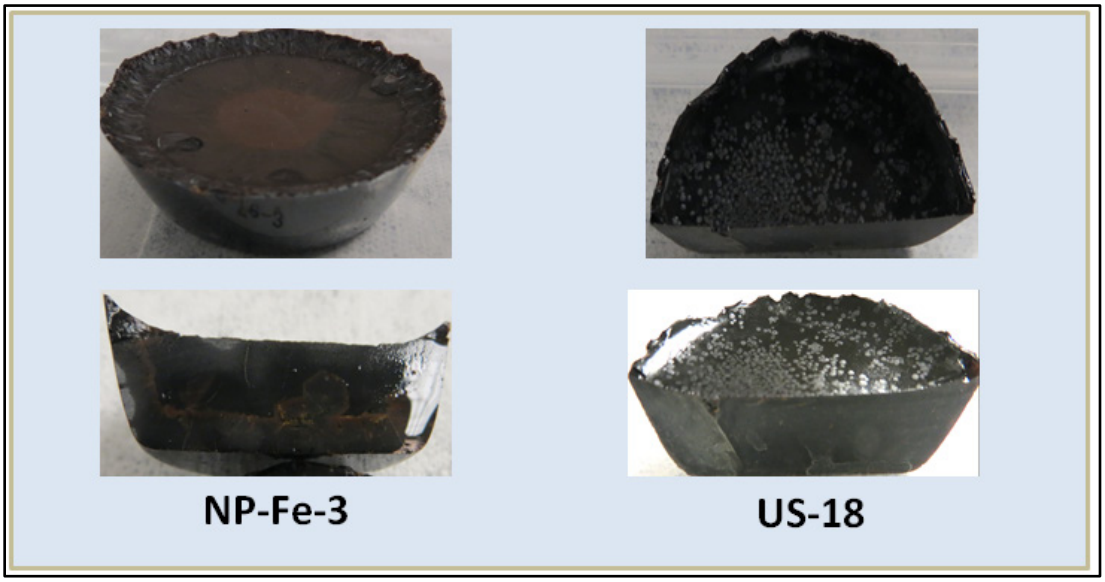

Figure 3-2. Photographs of glass subjected to heat treatment 2. Top: Glass-air interface. Bottom: Cross-sectional slice used for XRD.

Although the CCC, heat treatment 1 and heat treatment 2 results above provide valuable insight into the amount of nepheline expected to form as a function of time and temperature, the heat treatments cover a large temperature range and do not allow for identification of the specific portions of the heat treatments that are that most fostering of nepheline.

In an attempt to identify the specific portions of heat treatment 1 and 2 that might be driving nepheline formation, NP2-23 was selected to undergo cooling under the extreme slow (0.2 °C/min) and fast (2 °C/min) conditions seen in the thermal simulation data. NP2-23 was selected due to the relatively low amount of nepheline observed following heat treatment 1. It was hypothesized that this ND failing glass may potentially be made to form less than detectable limits of nepheline by only adjusting the time and temperature conditions of its cooling. Other glasses in this study, with the exception of US-18, exhibited

such large amounts of nepheline following heat treatment that the kinetic conditions needed to avoid the formation of nepheline may be unrealistic in a canister environment.

Once cooled from the melting temperature (1150 ℃) to one of the predetermined temperatures, NP2-23 was rapidly quenched to prevent additional crystallization from occurring. XRD was then measured and the results are shown in Table 3-2. Between 1150 ℃ and 850 ℃, under both fast (2.0 ℃/min) and slow (0.2 ℃/min) cooling conditions, the glass was X-ray amorphous. This result suggests two possibilities: either the crystalline phase formed in this temperature range is present at a concentration that is below XRD detection limits, or the liquidus temperature of this glass is below 850 ℃. The second possibility appears more likely since the DWPF spinel liquidus temperature model approximates a liquidus temperature of 855 ℃ for NP2-23.[20,21]

Table 3-2. XRD Results for NP2-23 Cooled Quickly and Slowly

Temperature Range of Heat Treatment	Phase(s) Identified (0.2 ℃/min cooling rate)	Phase(s) Identified (2.0 ℃/min cooling rate)
1150 ℃ - 950 ℃	Amorphous	Amorphous
1150 ℃ - 850 ℃	Amorphous	Amorphous
1150 ℃ - 750 ℃	Nepheline	Amorphous
1150 ℃ - 650 ℃	Nepheline	Amorphous
1150 ℃ - 550 ℃	Nepheline	Amorphous

Between 1150 ℃ and 750 ℃, nepheline was observed only under slow cooling conditions, thus suggesting, for the NP2-23 composition, that temperatures below 850 ℃ promote nepheline crystallization, a result confirmed by previous SRNL TTT work on other glass compositions[2] and the DWPF spinel liquidus temperature model.[3] However, the time spent below 850 ℃ appears to be an important factor. Specifically, the glass spent 50 minutes between 850 ℃ and 750 ℃ under the fast cooling conditions where no crystallization was seen, but spent 500 minutes in this range using the slow cooling rate. Therefore, to crystallize into a detectable amount, the glass needed to spend more than 50 minutes between 850 ℃ and 750 ℃. Similarly, between both 1150 ℃ and 650 ℃, and 1150 ℃ and 550 ℃, nepheline was detected in the slowly cooled samples, but the glass was amorphous under the fast cooling rate.

Under the fast cooling rate, the glass spent 250 and 300 min between 1150 ℃ - 650 ℃ and 1150 ℃ - 550 ℃, respectively. For the slow cooling rate, the glass spent 2500 and 3000 min between 1150 ℃ - 650 ℃ and 1150 ℃ - 550 ℃, respectively. Once again, the formation of nepheline under the slow cooling rate, and the lack of detectable amounts under the fast cooling rate, indicate nepheline formation in NP2-23 is not a fast process. Interestingly, this result contradicts earlier claims by Menkhaus et al.[22], who in 1999, stated that decreasing the nepheline content in a waste glass by faster cooling during glass production is unlikely due to the fast formation kinetics. This statement is in clear contradiction with the results presented herein for NP2-23, and warrants further investigation.

Importantly, from the data herein, it appears that nepheline is highly prone to form below 850 ℃, and that the lower temperature limit of the nepheline formation range seems to be, at most, 550 ℃. Thus, the length of time spent in the 850 ℃ to approximately 550 ℃ temperature range may be the prevailing factor as to why less nepheline was observed following heat treatment 2, where glass spent ~ 770 min in this range, than in heat treatment 1 and CCC where it spent ~ 870 and 1000 min respectively. It was later confirmed through additional heat treatment and DTA measurements that 550 ℃ does appear to be close to the lower limit of the nepheline formation temperature range (see below)

The formation of nepheline under slow cooling but not fast cooling also suggests the critical cooling rate needed to avoid nepheline formation is greater than 0.2 ℃/min but less than or equal to 2.0 ℃/min.

Evaluation of the entire canister simulation data shows that for heat treatment 1, the glass cools in the temperature range of 850 ℃ - 550 ℃ at a rate of approximately 0.34 ℃/min. In heat treatment 2 it cools through these temperatures at just a slightly higher rate of 0.38 ℃/min. The reheating of glass by subsequent glass pours following a pause in pouring is one reason why the cooling rate through this temperature range in heat treatment 2 is not faster. This point is illustrated in Figure 3-3, where the 850 ℃ – 550 ℃ temperature range in heat treatment 1 and 2 are highlighted. While the reheating of glass in heat treatment 1 occurs in a similar fashion as in heat treatment 2, the temperature region of this reheating is higher than 850 ℃ in heat treatment 1. However, this reheating in heat treatment 2 occurs within the 850 ℃ – 550 ℃ range, thus providing the glass extra time in this potentially problematic temperature zone.

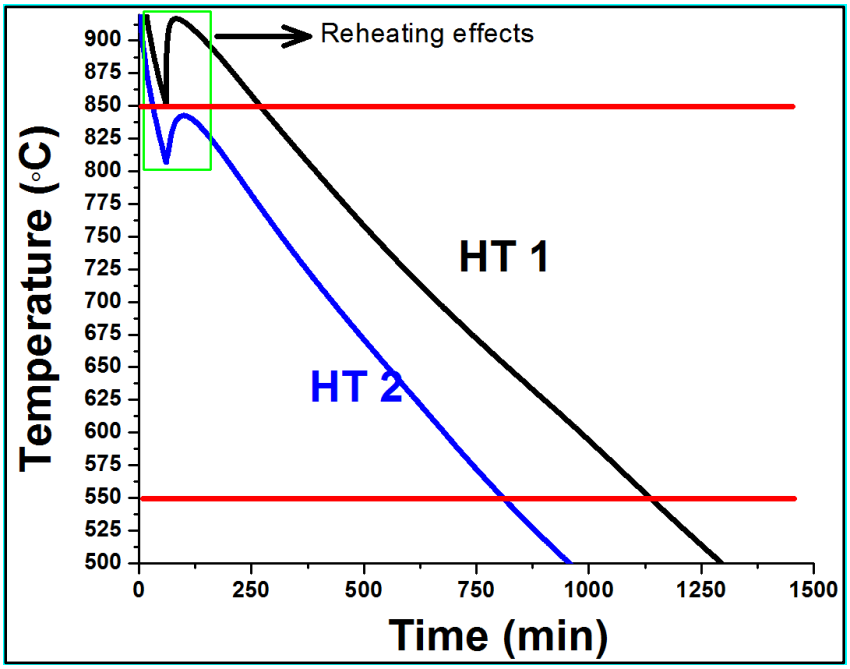

Figure 3-3. Reheating of glass from subsequent pours results in reheating of the already cooling glass. In heat treatment 2 this reheating occurs within the potentially problematic 850 ℃ - 550 ℃ temperature range, which is highlighted using the red lines.

This observation highlights the importance of the glass pour schedule in terms of providing accommodating time and temperature conditions for nepheline crystallization. For example, had the glass been poured continuously, rather than in intervals, the reheating from subsequent pours would likely not occur or would be greatly diminished, thus providing the glass with even less time in the potentially problematic temperature zone. However pouring continuously will have an impact on the cooling rate, which could be evaluated using the thermal model combined with laboratory work.

3.3 Differential Thermal Analysis of NP2-23

In an additional effort to become more focused on the exact time and temperature conditions that drive nepheline crystallization in NP2-23 glass, differential thermal analysis (DTA) on powder samples was measured up to 1000 ℃ at a 5 ℃ /min heating rate. The goal was to identify whether the DTA exothermic peaks represent the formation of crystalline phases, and whether DTA can be used as a quick probe to determine the temperatures of crystallization in a waste glass simulant. The measurements consistently exhibited 3 exothermic peaks, assumed to be associated with crystal phase formation, at approximately 601 ℃, 715 ℃, and 776 ℃ as shown in Figure 3-4.

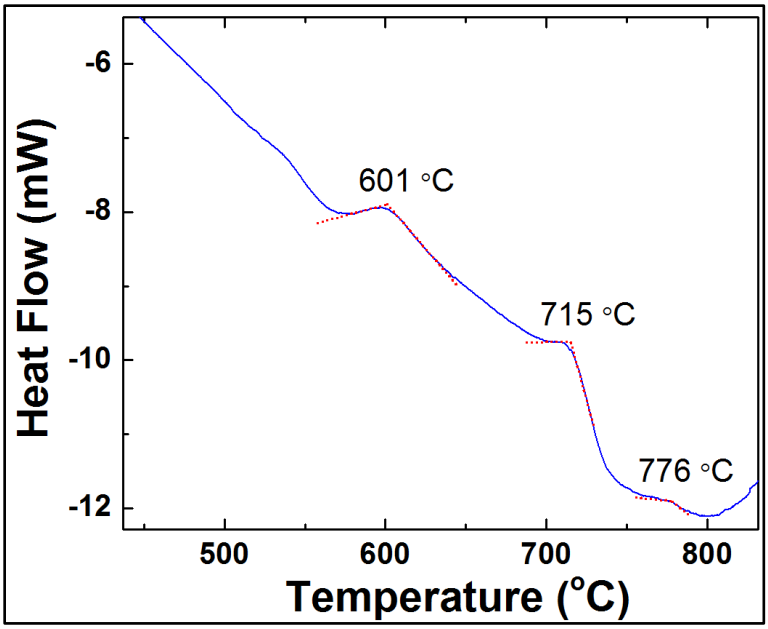

Figure 3-4. DTA thermogram of NP2-23 using a heating rate of 5 °C/min.

Using the DTA data as a guide for the temperatures of crystal formation, 5 g of crushed NP2-23 was held for 24 hours at 500 °C, 600 °C, 750 °C, 850 °C, and 950 °C, and was quenched after these holds. The small sample volume was used to replicate the glass surface/volume conditions in a DTA measurement, thus while a representative piece of each sample was obtained following heat treatment, the sampling method may be slightly different than described in Section 2.6.1. OM and SEM images as well as EDS measured elemental maps for each sample are presented below. The XRD data for these samples is provided in Table 3-3. These data correlate well with those in Table 3-2, yet the temperatures of interest were approached from different directions (heating up in Table 3-3 and cooling down in Table 3-2)

According to the XRD results, NP2-23 is amorphous after heat treatment at 950 °C and 500 °C, but shows nepheline at 850 °C and 750 °C, and nepheline + lithium silicate at 600 °C. The observation of an amorphous structure after heat treatment at 500 °C suggests that this temperature is below the lower limit of the nepheline formation range. It was not possible to interpret the DTA data using XRD alone, thus OM and SEM were used as additional aids.

Table 3-3. XRD Results for 24 hr. Isothermal Heat Treatment of NP2-23

Temperature of 24hr Isothermal Hold	Phase(s) Identified
500 °C	Amorphous
600 °C	Nepheline Lithium Silicate (Li_2SiO_3)
750 °C	Nepheline
850 °C	Nepheline
950 °C	Amorphous

OM images of NP2-23 following heat treatment at 500 °C, 600 °C, 750 °C, 850 °C and 950 °C are provided in Figure 3-5. The images appear to show the glass as crystal-free following treatment at 500 °C, however, after 24 hrs. at 600 °C the glass appears to have dark needle/star-like crystals. At 750 °C the glass appeared to have small shapeless dark crystals. At 850 °C it appeared to have small shapeless dark

crystals in addition to large tetragonal-like transparent crystals. At 950 ℃ the glass appears to be crystal-free.

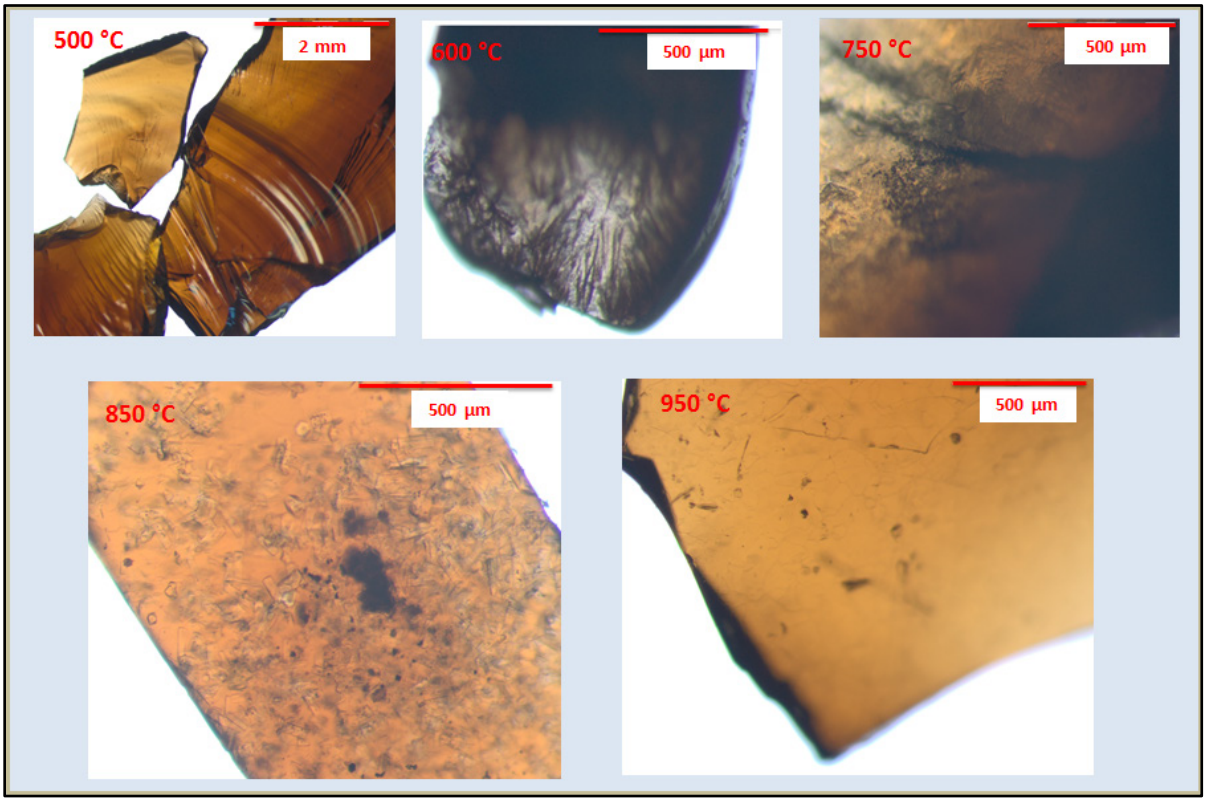

Figure 3-5. Optical microscopy images of NP2-23 showing the formation of different crystalline phases after a 24 hr. heat treatment at 600 ℃, 750 ℃ and 850 ℃. The glass was amorphous after 24 hrs. at 500 ℃ and 950 ℃, thus suggesting the primary temperature range for crystal formation (T) is 500<T<950.

The lack of crystal formation after treatment at 500 ℃ is likely due to this temperature being close to or below the NP2-23 glass transition temperature. It was observed, following this treatment, that the glass did not appear to melt and was therefore, likely left in its quenched state. The lack of crystal formation after the 950 ℃ treatment is likely due to the liquidus temperature of NP2-23 being below this temperature, a result that is supported by the DWPF spinel liquidus temperature model, which predicts a liquidus temperature of 855 ℃ for NP2-23. The lack of crystallization at 500 ℃ and 950 ℃ is in agreement with the lack of DTA peaks seen below 600 ℃ or above 800 ℃. Additionally, the 950 ℃ result is in agreement with the observation of an X-ray amorphous structure after heat treatment between 1150 ℃ and 950 ℃ as shown in Table 3-2.

SEM/EDS were employed in an effort to identify the crystallites seen in the OM images of 600 ℃, 750 ℃, and 850 ℃ heat treated glass. The SEM and EDS elemental map for the 600 ℃ glass are displayed in Figure 3-6. In these data, a needle/star-like phase was observed. This phase contains Al, Si, and Na, thus suggesting that it might be nepheline, which agrees with XRD data. The 750 ℃ data in Figure 3-7 clearly show the presence of Cr, Mn, Fe and Ni-based crystals which are likely spinels ((Fe, Ni, Mn, Zn)$(Fe,Cr)_2O_4$) that were too low in concentration to detect using XRD. There also seems to be a Mg/Ca-rich phase present and possibly some nepheline, although nepheline is the only phase abundant enough to be detected by XRD. Importantly, because Ca and Mg can substitute into the nepheline structure, the Mg/Ca phase is tentatively attributed to substituted nepheline. At 850 ℃, the data (Figure 3-8) show a

large Al, Na, Si based crystal, which is likely nepheline that was also seen in XRD. Additionally, small spinel-like crystals are again observed, although they were not seen in XRD. These results seem to indicate that the abundant transparent crystals seen in the OM image of the 850 ℃ glass correspond to nepheline, while the less abundant dark crystals are likely spinels at a concentration below the XRD detection limits.

In an attempt to relate XRD, OM, and SEM observations to DTA, it can be tentatively stated that the first exothermic peak in DTA corresponds to formation of either the needle/star-like nepheline phase found from EDS and XRD or lithium silicate found only from XRD. The second exothermic peak at 715 ℃ seems to correspond to the formation of spinel phases, which are prominently seen in the EDS following 24 hour heat treatment at 750 ℃. Lastly, the origin of the third exothermic peak is not clear, but may result from an undetected phase or from nepheline, which appears to be the plentiful transparent crystalline phase observed in OM and SEM for glass heat treated for 24 hours at 850 ℃. While analysis of the DTA results is subject to further interpretation at this stage, the results do seem to indicate that DTA is a viable tool for quickly probing waste glass simulants for the temperatures at which crystallization occurs during a specific heating treatment. However, it is necessary to use other tools such as EDS and XRD to help identify the type of crystallization represented by a DTA exotherm.

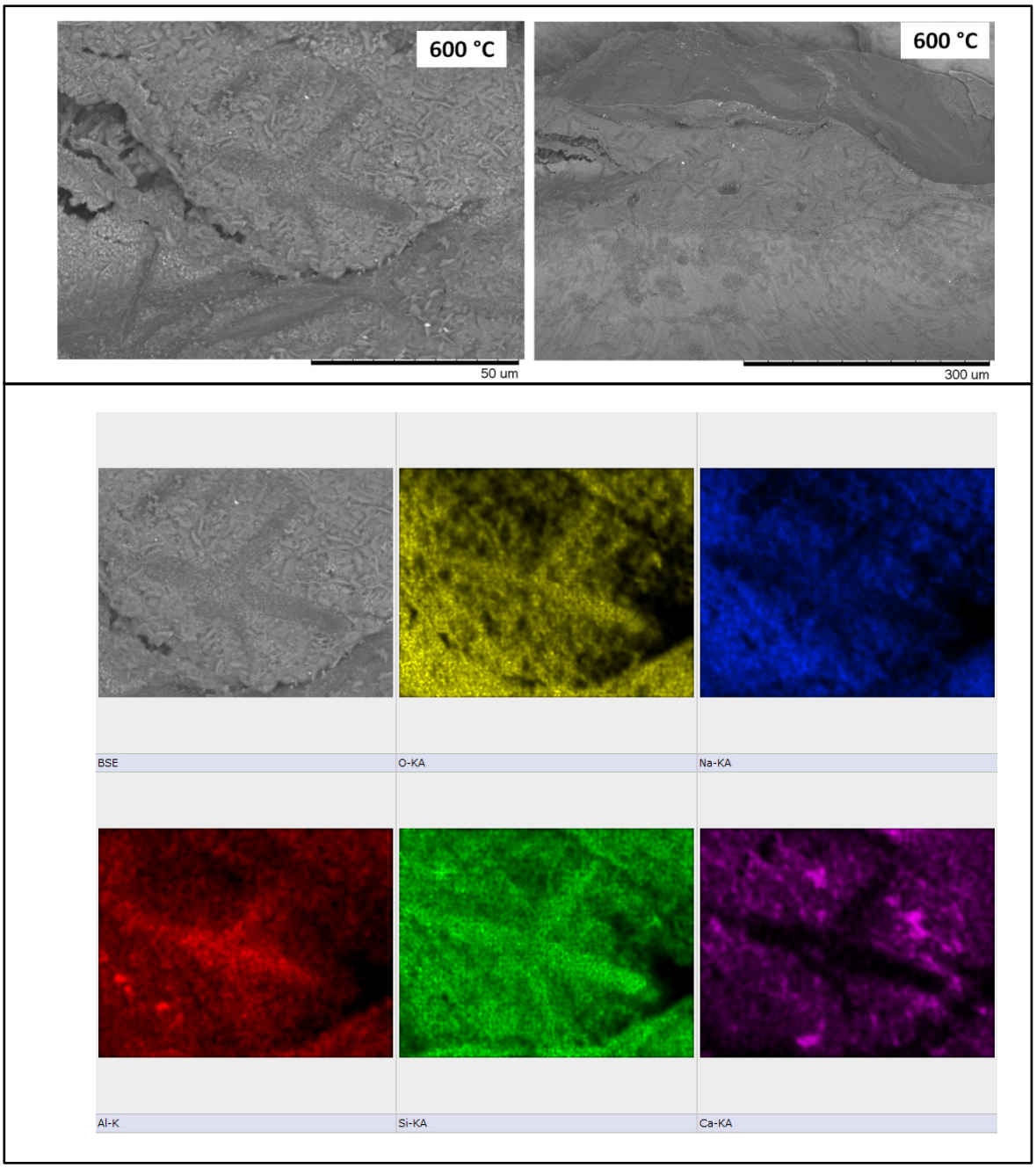

Figure 3-6. Top: SEM images of NP2-23 after a 24 hr. heat treatment at 600 ℃. Bottom: The EDS elemental map shows a large spinel crystal containing Mn, Ni, Fe, and Cr with no Si. The needle shaped materials appear to be nepheline with Mg and Ca substitution.

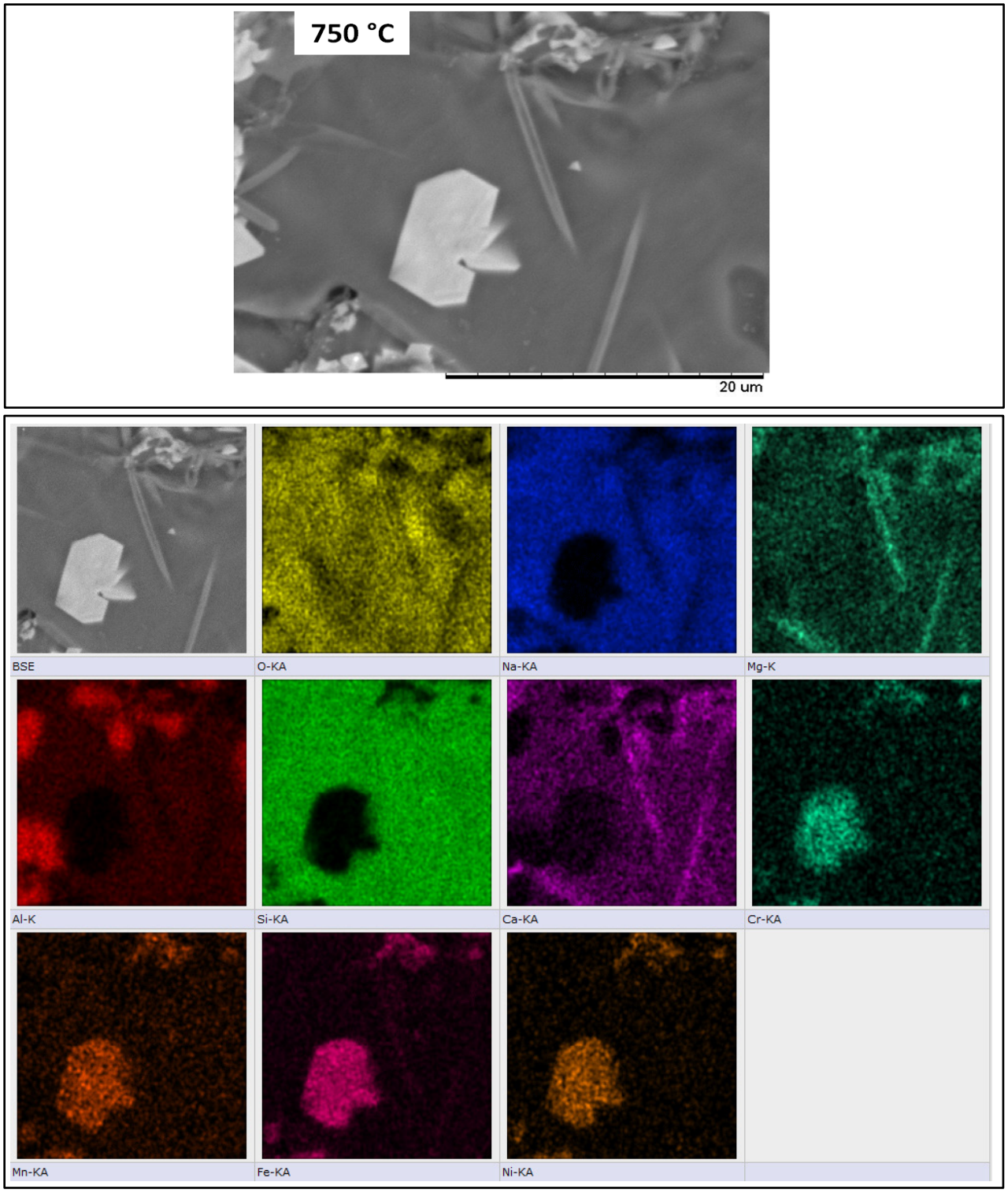

Figure 3-7. Top: SEM image of NP2-23 after 24 hr. heat treatment at 750 ℃. The elemental map on the bottom shows evidence of a large Cr, Mn, Fe, and Ni containing crystal, which is likely a spinel ($(Fe, Ni, Mn, Zn)(Fe,Cr)_2O_4$) phase. There also appears to be nepheline in the top right portion of the image.

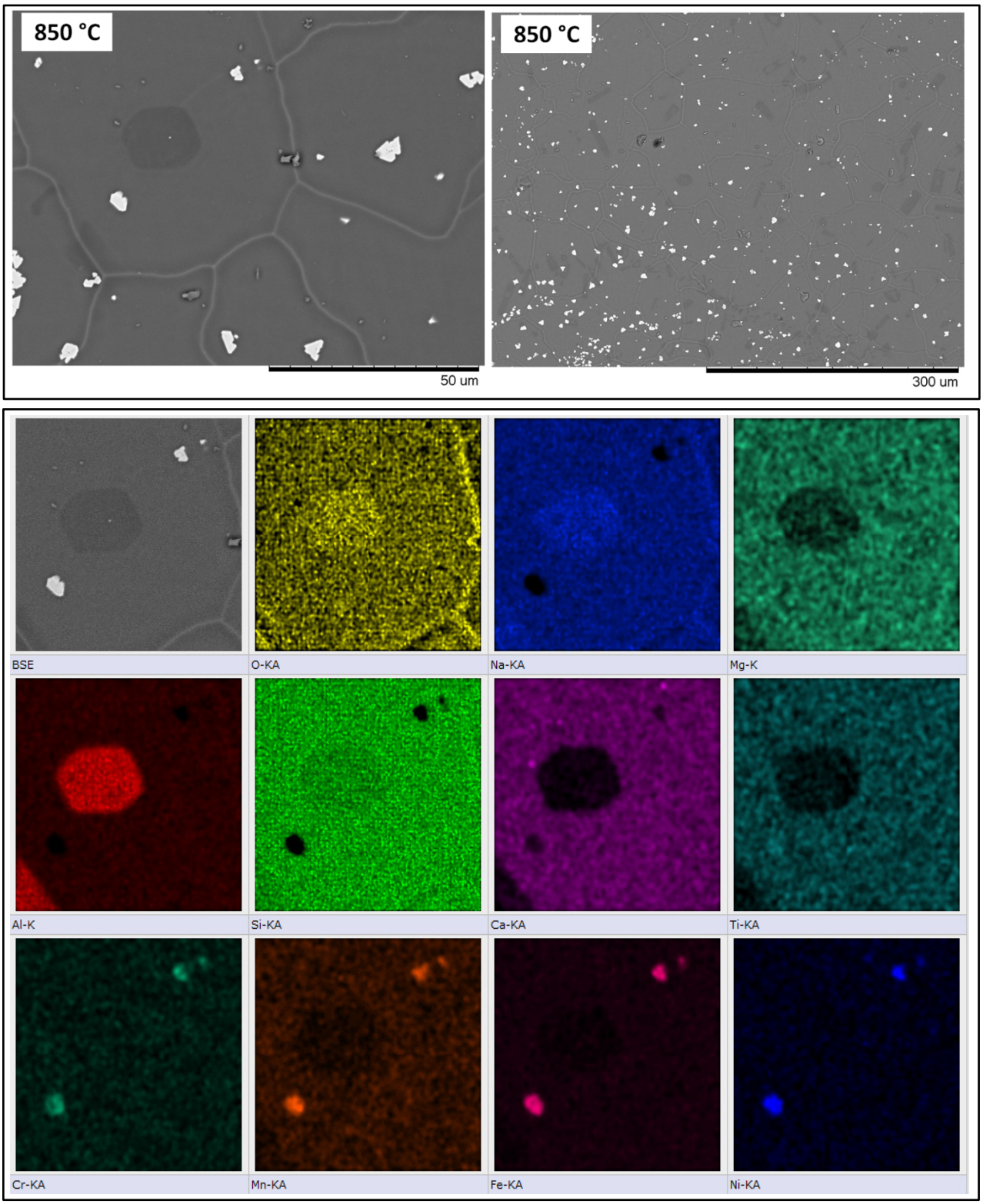

Figure 3-8. Top: SEM image of NP2-23 after 24 hr. heat treatment at 850 ℃. The elemental map on the bottom shows several small Cr, Mn, Fe, and Ni containing spinel crystals and a large hexagonal crystal, which is tentatively ascribed to nepheline, but may be an undissolved Al_2O_3 particle based on the lack of Si in the material.

4.0 Conclusions and Path Forward.

Five glass compositions were selected in order to study the role of kinetics in nepheline formation. Each glass was subjected to the time and temperature conditions present at the 1 in. offset from canister centerline position during a pour schedule utilizing 29 min pours and 58 min pauses between pours. Two glasses were subjected to conditions at the 6 in. offset from centerline position under a similar pour schedule. The studied glasses were fairly broad in compositional space and covered ND values from 0.48 – 0.60. The primary crystalline phase detected in each glass after heat treatment was nepheline, although the concentration depended on the cooling rate, which is dependent both on the position within the canister that the glass cools, and the glass pour schedule. Further studies are recommended to evaluate a quantitative relationship between cooling rate and nepheline concentration as a function of glass composition, although it can tentatively be stated that nepheline concentration should decrease the further that glass cools from the centerline.

For composition NP2-23, cooling at a rate of 2.0 ℃/min was sufficient for preventing nepheline crystallization; however, cooling at 0.2 ℃/min resulted in nepheline formation. It is thus believed that the critical cooling rate needed to prevent nepheline crystallization is greater 0.2 ℃/min but less than or equal to 2.0 ℃/min. Additionally, for NP2-23, the 850 ℃ - 550 ℃ temperature range appears to be accommodating towards nepheline formation while temperatures above 850 ℃ are not, and temperatures below 500 ℃ are not. Evaluation of the canister thermal simulations showed that, on average, glass spends ~770 min in this range at the 6 in. offset position and ~870 min in this range at the 1 in. offset position. The glass spends a negligible portion of its time (directly after pouring only) in this temperature range at the 12 in. offset position, thus the probability for nepheline crystallization at the canister walls should be near 0. It is suggested that computer simulations be developed to determine the exact volume of glass in a canister that cools under particular cooling rates. These results would help to determine the volume of nepheline expected in a waste canister once it has cooled.

The reheating of glass by subsequent glass pours, following a pause in pouring, was found to increase the amount of time that glass spends between 850 ℃ – 550 ℃ at the 6 in. offset from centerline position, but not at the 1 in. offset position. This observation highlights the importance of the glass pour schedule in terms of providing accommodating time and temperature conditions for nepheline crystallization.

DTA measurements of NP2-23 were proven useful for quickly evaluating the temperature range(s) in which crystallization is likely to occur, although identification of the crystalline phase corresponding to DTA exotherms requires additional tools like EDS and XRD.

It is recommended that additional glass compositions be subjected to the 1 in. offset and 6 in. offset from centerline cooling conditions in order to create a database that relates the nepheline concentration to the cooling rate and the glass compositions. Additionally, small interval cooling rate experiments, like the one described herein, should be performed for NP2-23 between 850 ℃ and 550 ℃ at cooling rates greater than 0.2℃ but less than 2.0 ℃. Similar studies are recommended for other glass compositions in order to determine whether a universal critical cooling rate exists for preventing nepheline crystallization.

Finally, with the knowledge obtained from these studies, that show time and temperature conditions are crucial towards nepheline formation, it is recommended that strategies be developed to increase the cooling rate of glass within a canister. It may be possible to achieve faster cooling by flowing cold air over the glass or canister as it cools, by adjusting the glass pouring schedule, or by pouring glass into a rotating canister that utilizes centrifugal force to rapidly push glass to the cooler canister walls. Other strategies unforeseen at this time might also be possible.

5.0 References.

1. Schiebold, E., On the Structure of Nepheline and Analcite. *Naturwiss* **1930,** *18*, 705.
2. Jantzen, C. M.; Bickford, D. F., Leaching of Devitrified Glass Containing Simulated SRP Nuclear Waste. *Sci. Basis for Nuclear Waste Management VIII, C.M. Jantzen, J. A. Stone, R. C. Ewing (eds), Materials Research Society, Pittsburgh, PA 135-146* **1985**.
3. Marra, S. L.; Andrews, M. K.; Cicero, C. A., Phase Stability Determinations of DWPF Waste Glasses. *WSRC-TR-93-00227, Rev. 0* **1993**.
4. Li, H.; Jones, B.; Hrma, P.; Vienna, J. D., Compositional Effects on Liquidus Temperature of Hanford Simulated High-Level Waste Glasses Precipitating Nepheline (NaAlSiO4). *Environmental Issues and Waste Management Technologies in the Ceramic and Nuclear Industries, III, D. K. Peeler and J. C. Marra (Eds.), Am. Ceram. Soc., Westerville, OH, 279-288* **1998**.
5. Li, H.; Hrma, P.; Vienna, J. D.; Qian, M.; Su, Y.; Smith, D. E., Effects of Al_2O_3, B_2O_3, Na_2O, and SiO_2 on Nepheline Formation in Borosilicate Glasses: Chemical and Physical Correlations. *J. Non-Cryst. Solids* **2003,** *331*, 202-216.
6. Li, H.; Vienna, J. D.; Hrma, P.; Smith, D. E.; Schweiger, M. J., Nepheline Precipitation in High-Level Waste Glasses: Compositional Effects and Impact on the Waste Form Acceptability. *Proceedings of MRS* **1997,** *465* (Scientific Basis for Nuclear Waste Management).
7. Edwards, T. B.; Peeler, D. K.; Fox, K. M., The Nepheline Discriminator: Justification and DWPF PCCS Implementation Details. *U.S. Department of Energy Report WSRC-STI-2006-00014, Revision 0* **2006,** *Washington Savannah River Company, Aiken, SC.*
8. Fox, K. M.; Edwards, T. B., Refinement of the Nepheline Discriminator: Results of a Phase I Study. *SRNS-STI-2008-00099, Rev. 0.*
9. Fox, K. M.; Edwards, T. B., Refinement of the Nepheline Discriminator: Results of a Phase II Study. **2008,** *SRNS-STI-2008-00099, Rev. 0.*
10. Fox, K. M.; Edwards, T. B., Experimental Results of the Nepheline Phase III Study. *SRNL-STI-2009-00608, Rev. 0* **2009**.
11. McCloy, J. S.; Schweiger, M. J.; Rodriguez, C. P.; Vienna, J. D., Nepheline Crystallization in Nuclear Waste Glasses Progress Toward Acceptance of High-Alumina Formulations. *Int. J. Appl. Glass Sci* **2011,** *2*, 201-214.
12. Amoroso, J. W., The Impact of Kinetics on Nepheline Formation in Nuclear Waste Glasses. *SRNL-STI-2011-00051, Rev. 0* **2011**.
13. Deer, W. A.; Howie, R. A.; Zussman, J., *Rock-Forming Minerals*. John Wiley & Sons, Inc., NY, 435pp: 1963; Vol. 4.
14. Klingenberg, R.; Felsche, J., Interstitial Cristobalite-type Compounds $(Na_2O)_{0.33}Na[AlSiO_4]$. *J. Solid State Chemistry* **1986,** *61*, 40-46.
15. Hrma, P., Crystallization during processing of nuclear waste glass. *Journal of Non-Crystalline Solids* **2010,** *356* (52–54), 3019-3025.
16. Email Communication from Jarod Crum, P. N. N. L., April 10, 2014.
17. Fox, K. M.; Peeler, D. K.; Edwards, T. B.; Best, D. R.; Reamer, I. A.; Workman, R. J.; Marra, J. C.; Riley, B. J.; Vienna, J. D.; Crum, J. V.; Matyas, J.; Edmondson, A. B.; Lang, J. B.; Ibarra, N. M.; Fluegel, A.; Aloy, A. S.; Trofimenko, A. V.; Soshnikov, R., International Study of Aluminum Impacts on Crystallization in U. S. High Level Waste Glass. *U. S. Department of Energy Report SRNS-STI-2008-00057, Revision* **2008,** *Savannah River National Laboratory, Aiken, SC, .*
18. Kesterson, M. R., COMSOL Multiphysics Model for HLW Canister Filling, Revision 0. *SRNL-STI-DRAFT, Rev 0* **December 8, 2014**.
19. Marra, S. L.; Jantzen, C. M.; Ramsey, A. A., DWPF Glass Transition Temperatures - What They Are And Why They Are Important (U). *WSRC-MS-91-112* **1991**.
20. Jantzen, C. M.; Brown, K. G., Predicting the spinel-nepheline liquidus for application to nuclear waste glass processing. Part I: Primary phase analysis, liquidus measurment, and quasicrystalline approach. *J. Am. Ceram. Soc.* **2007,** *90* (6), 1866-1879.

21. Jantzen, C. M.; Brown, K. G., Predicting the spinel-nepheline liquidus for application to nuclear waste glass processing. Part II: Quasicrystalline freezing point depression model. *J. Am. Ceram. Soc.* **2007,** *90* (6), 1880-1891.
22. Menkhaus, T. J.; Hrma, P.; Li, H., Kinetics of Nepheline Crystallization From High-Level Waste Glass. In *Ceramic Transactions*, Chandler, G. T.; Feng, X., Eds. Ceramic Transactions: Westerville, OH, 1999; Vol. 107.

6.0 Appendix

XRD of Glasses Subjected To Canister Simulation Heat Treatment:

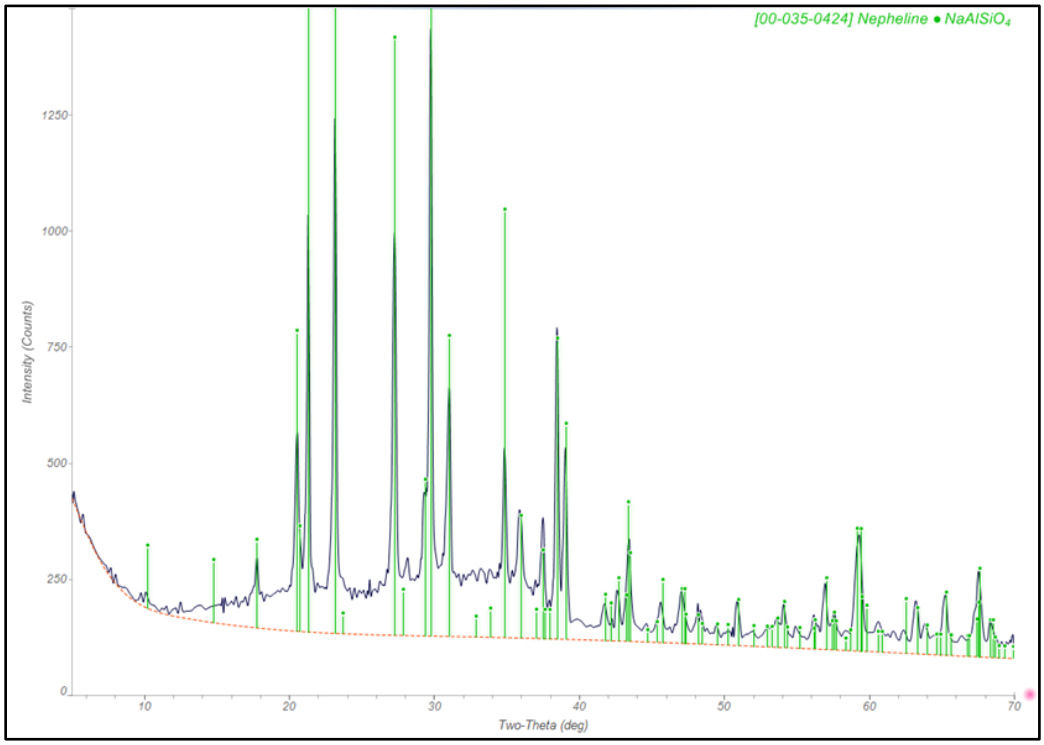

Figure A-1. X-ray diffraction pattern of NP-Fe-3 after heat treatment 1

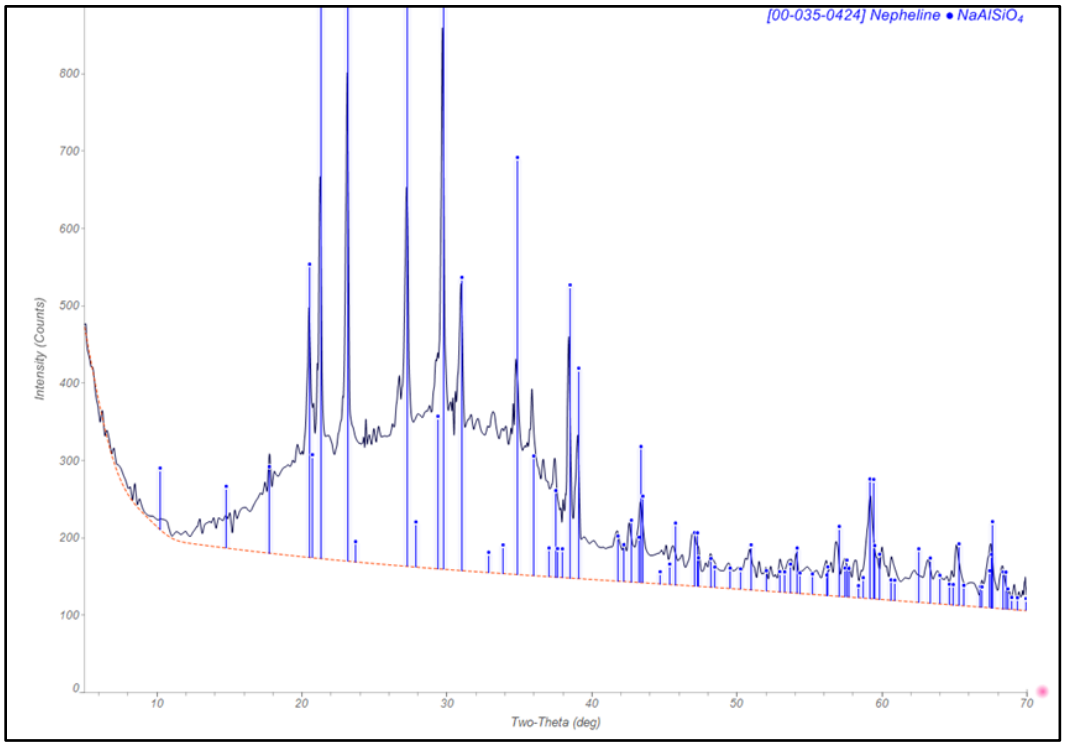

Figure A-2. X-ray diffraction pattern of NP-Fe-3 after heat treatment 2

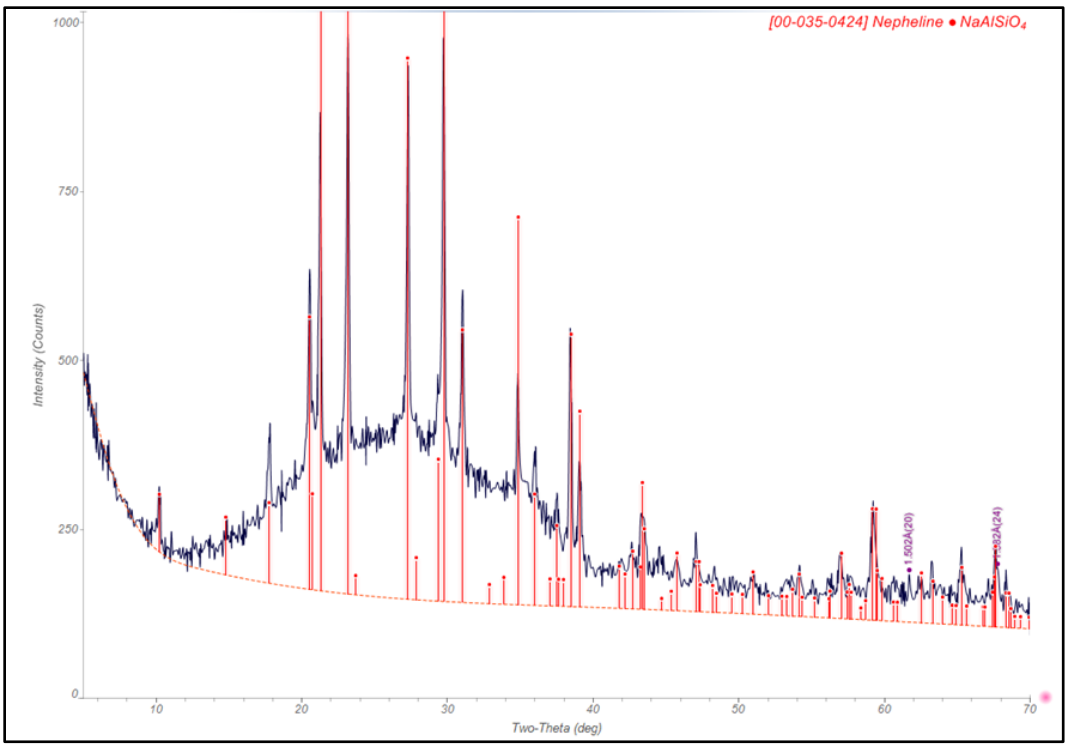

Figure A-3. X-ray diffraction pattern of US-18 after heat treatment 1

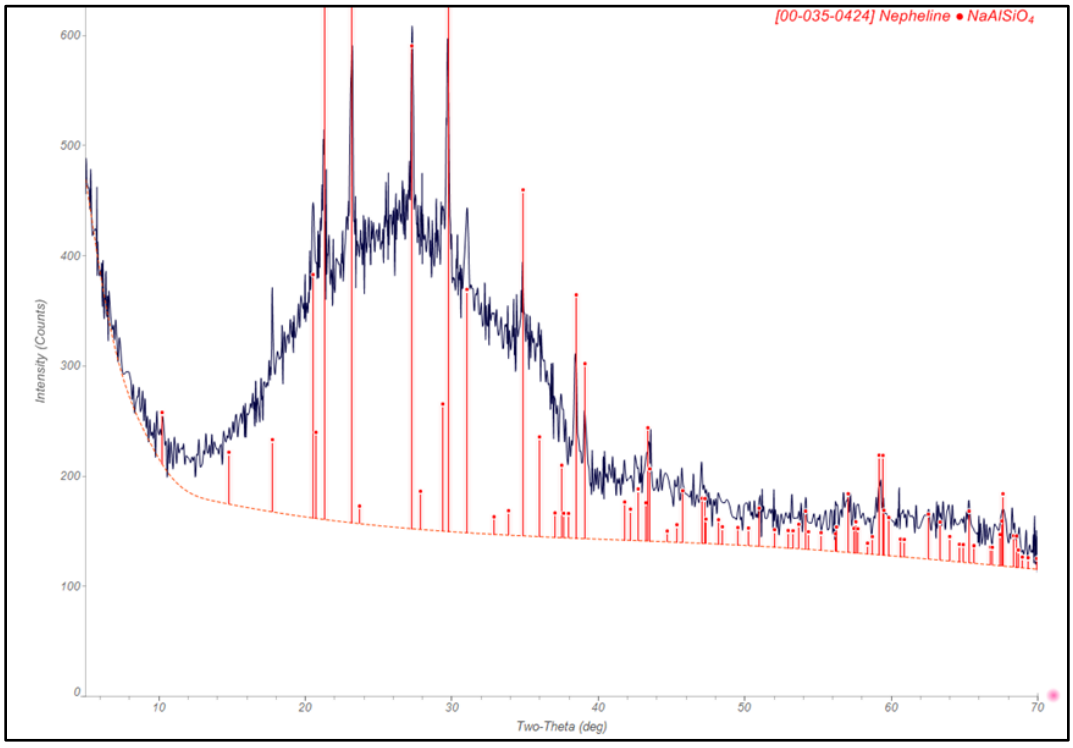

Figure A-4. X-ray diffraction pattern of US-18 after heat treatment 2

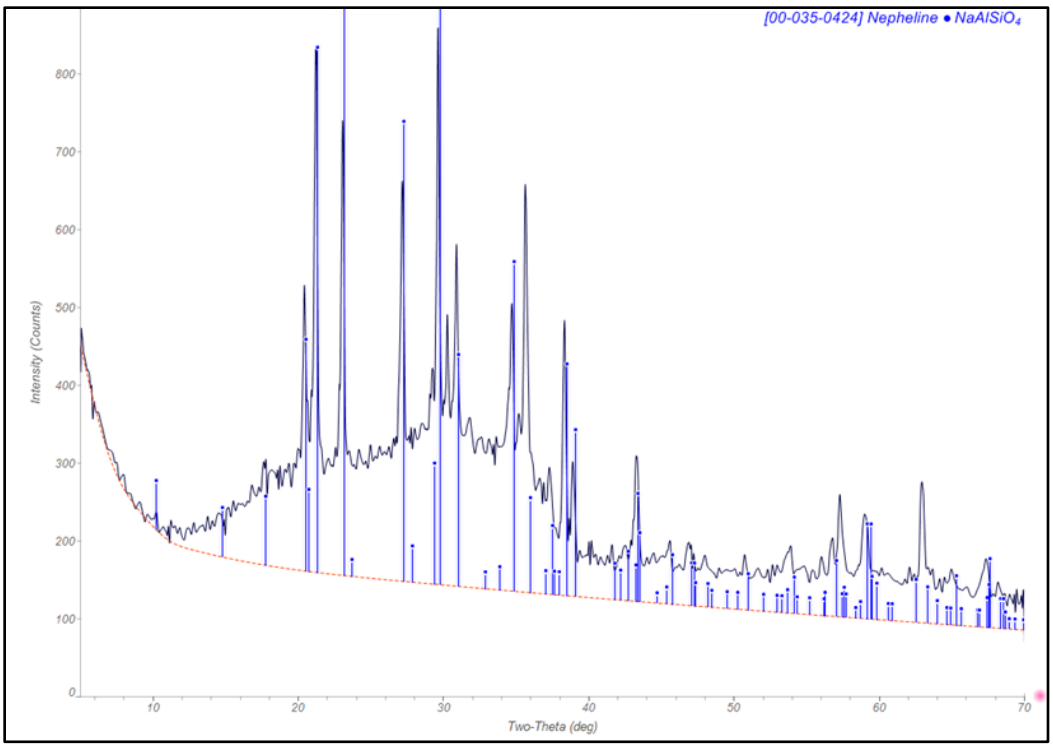

Figure A-5. X-ray diffraction pattern of US-37 after heat treatment 1

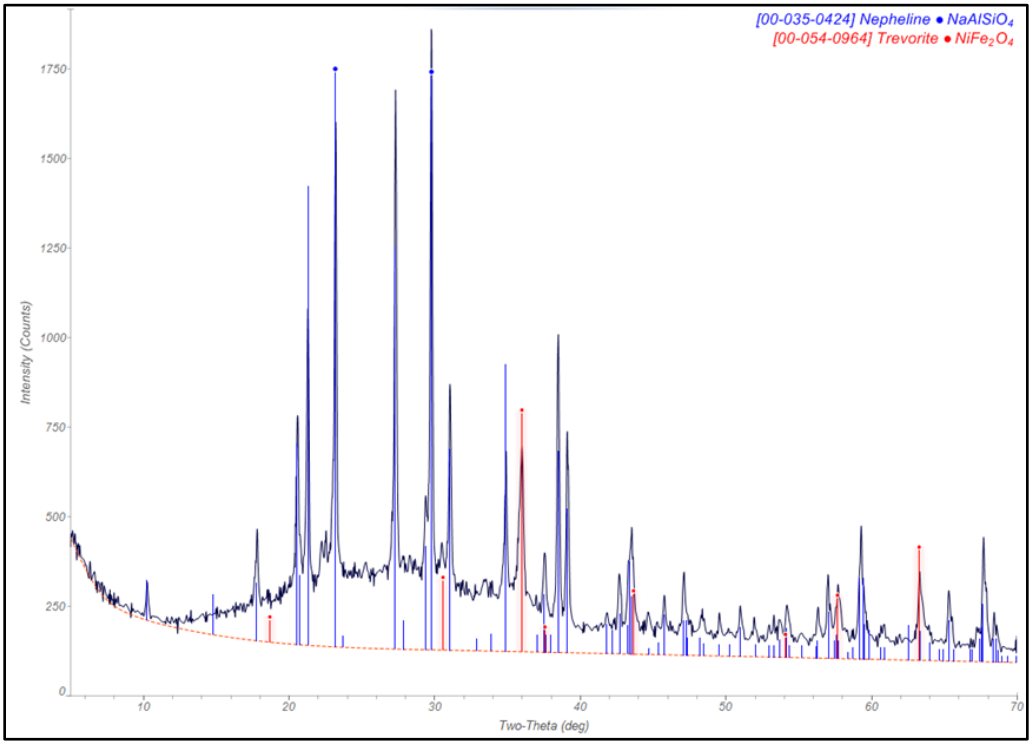

Figure A-6. X-ray diffraction pattern of A4 after heat treatment 1

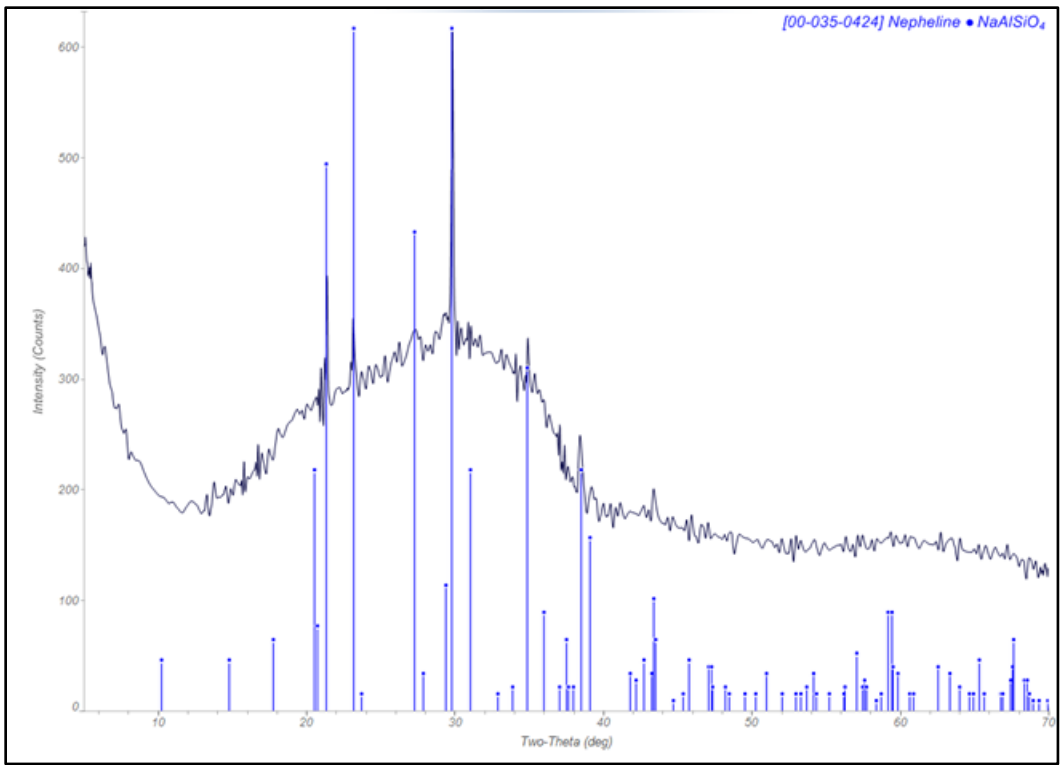

Figure A-7. X-ray diffraction pattern of NP2-23 after heat treatment 1

XRD Patterns of Glass Composition, NP2-23, Cooled Under Extreme Slow and Fast Conditions:

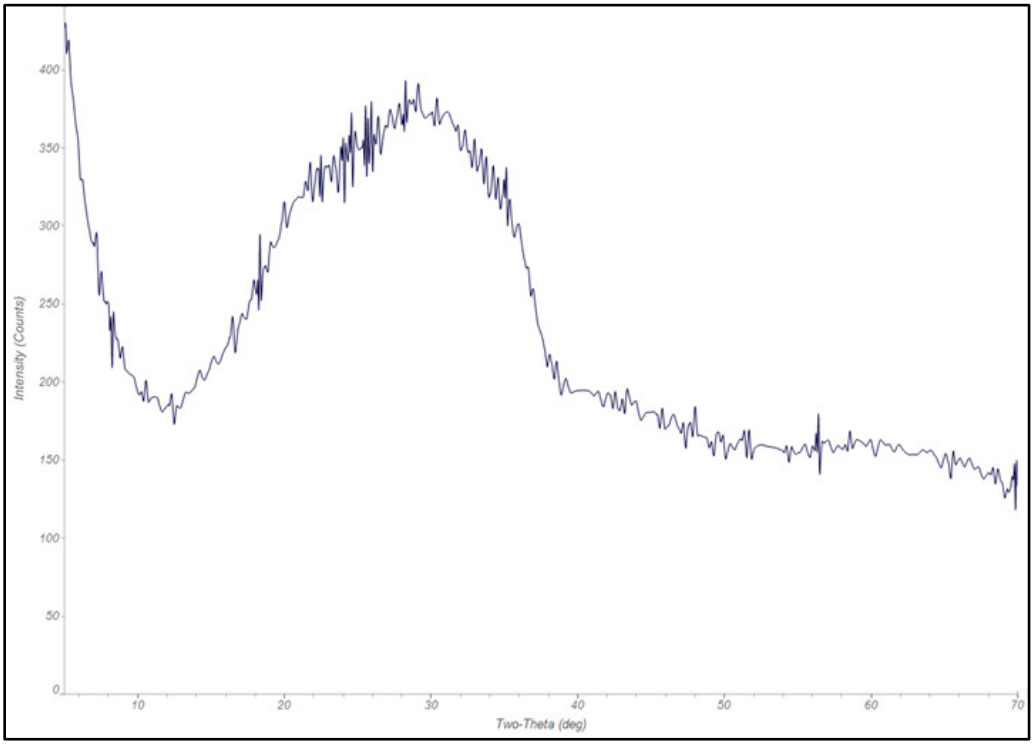

Figure A-8. X-ray diffraction pattern of NP2-23 cooled between 1150 ℃ and 950 ℃ at 0.2℃/min

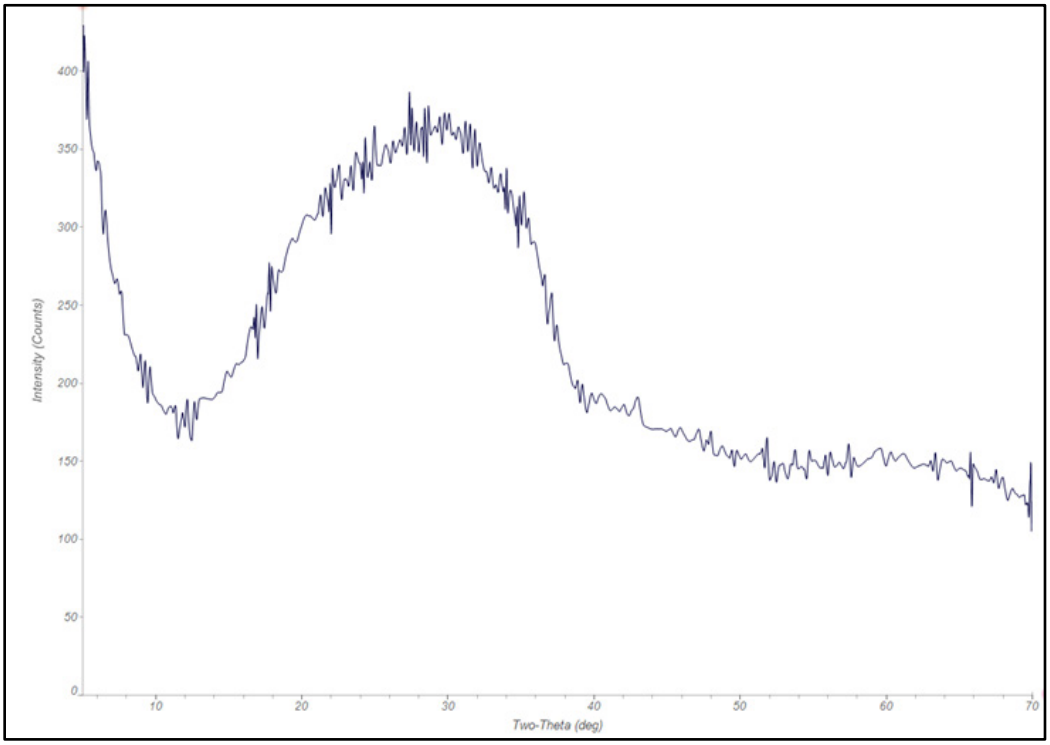

Figure A-9. X-ray diffraction pattern of NP2-23 cooled between 1150 ℃ and 850 ℃ at 0.2℃/min

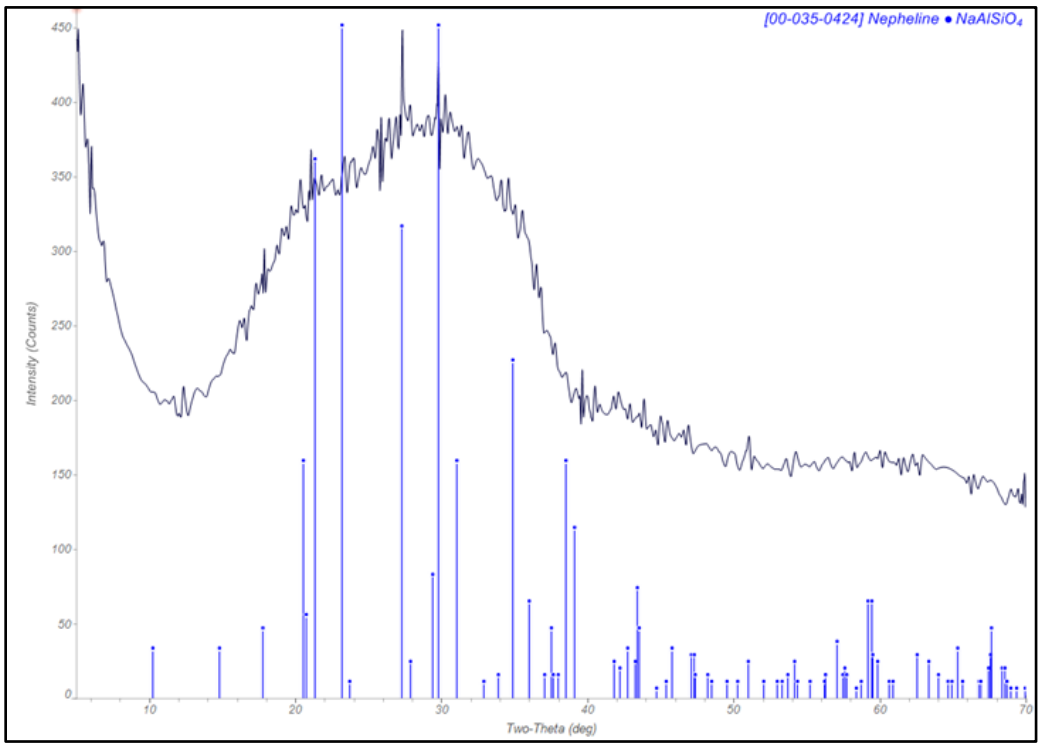

Figure A-10. X-ray diffraction pattern of NP2-23 cooled between 1150 ℃ and 750 ℃ at 0.2℃/min

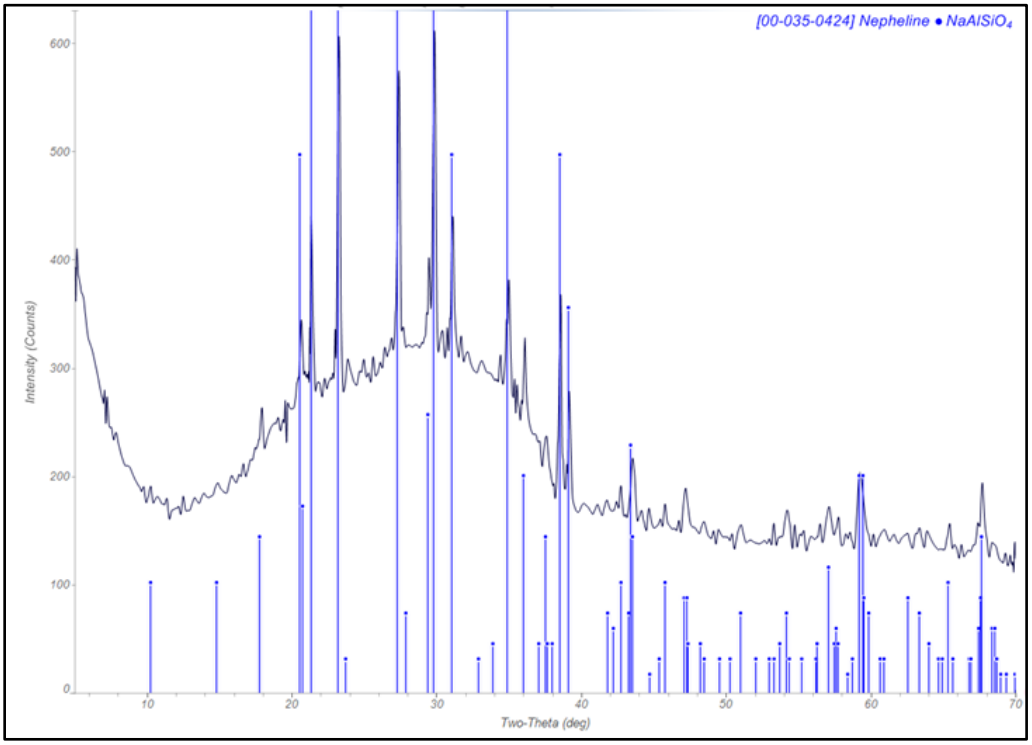

Figure A-11. X-ray diffraction pattern of NP2-23 cooled between 1150 ℃ and 650 ℃ at 0.2℃/min

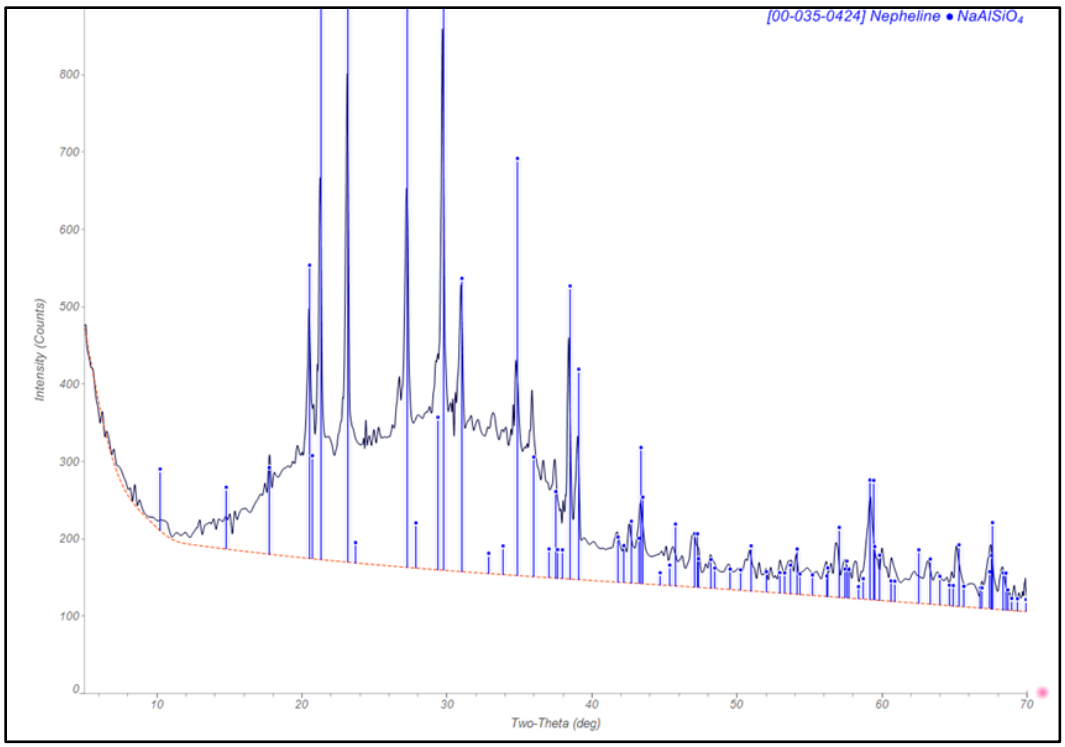

Figure A-12. X-ray diffraction pattern of NP2-23 cooled between 1150 ℃ and 550 ℃ at 0.2℃/min

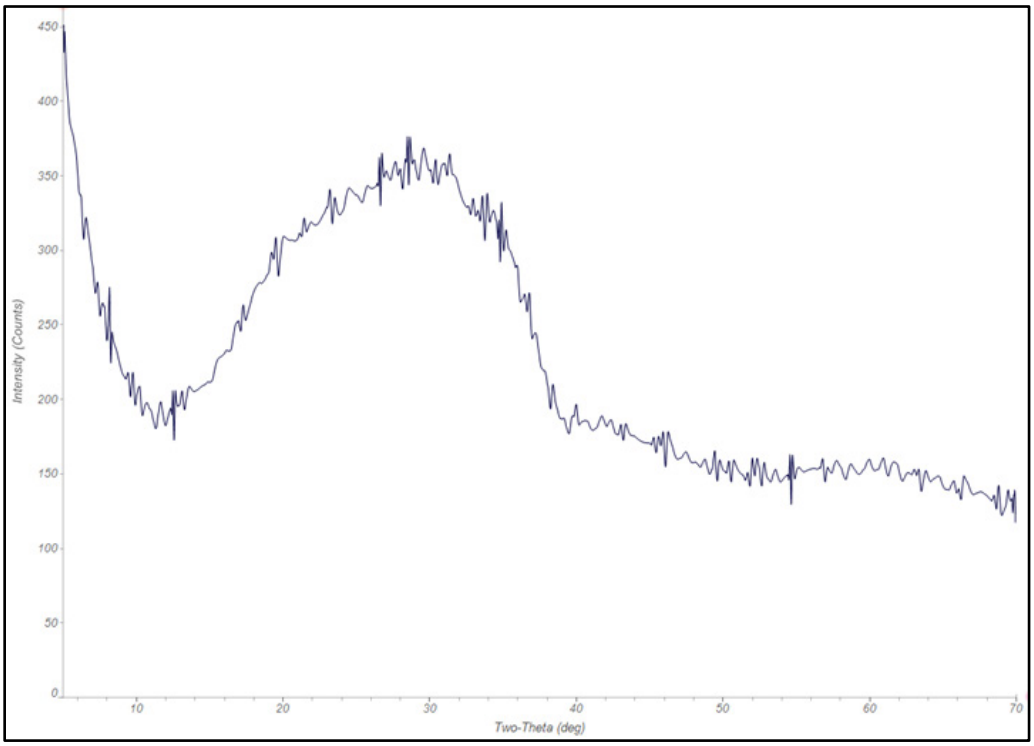

Figure A-13. X-ray diffraction pattern of NP2-23 cooled between 1150 ℃ and 950 ℃ at 2.0℃/min

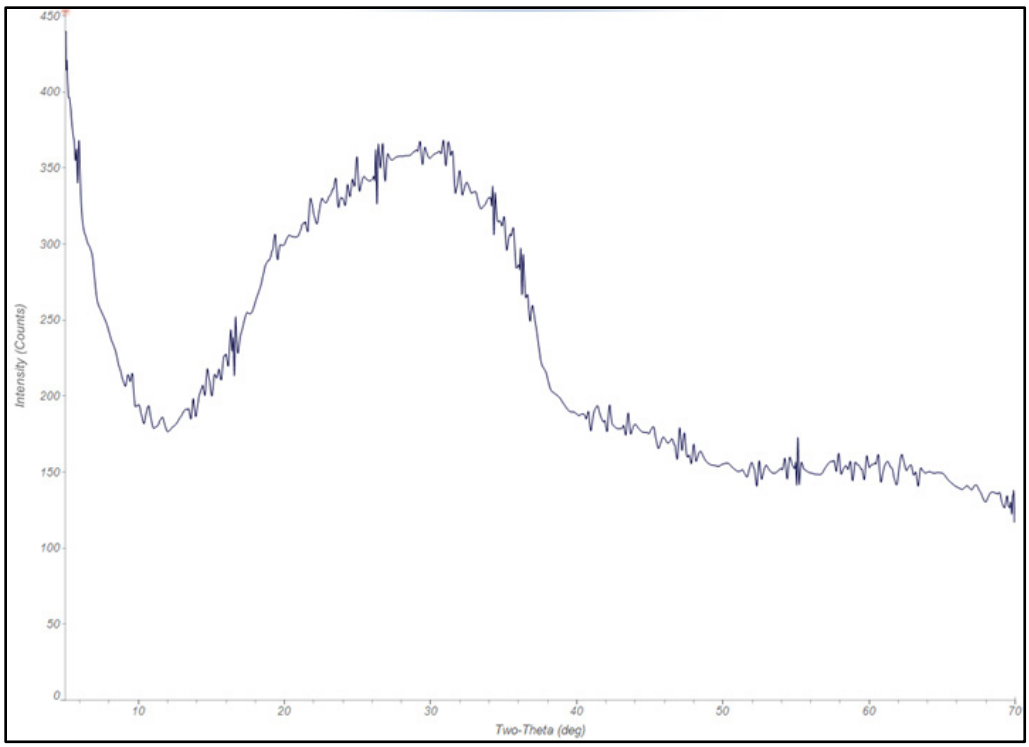

Figure A-14. X-ray diffraction pattern of NP2-23 cooled between 1150 ℃ and 850 ℃ at 2.0℃/min

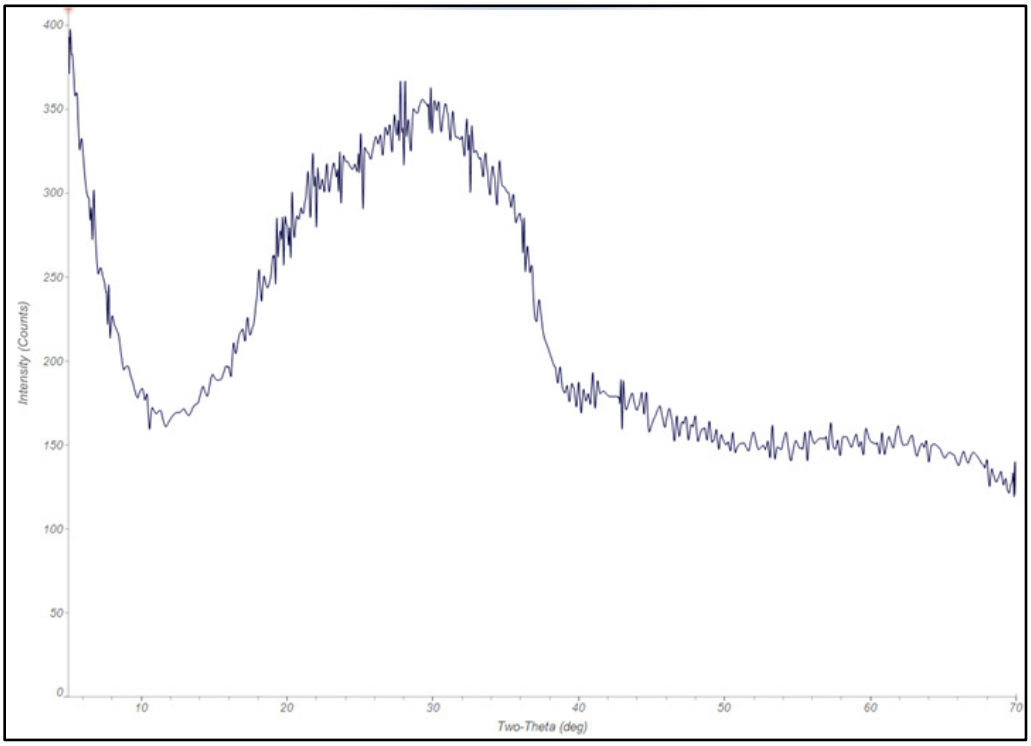

Figure A-15. X-ray diffraction pattern of NP2-23 cooled between 1150 ℃ and 750 ℃ at 2.0℃/min

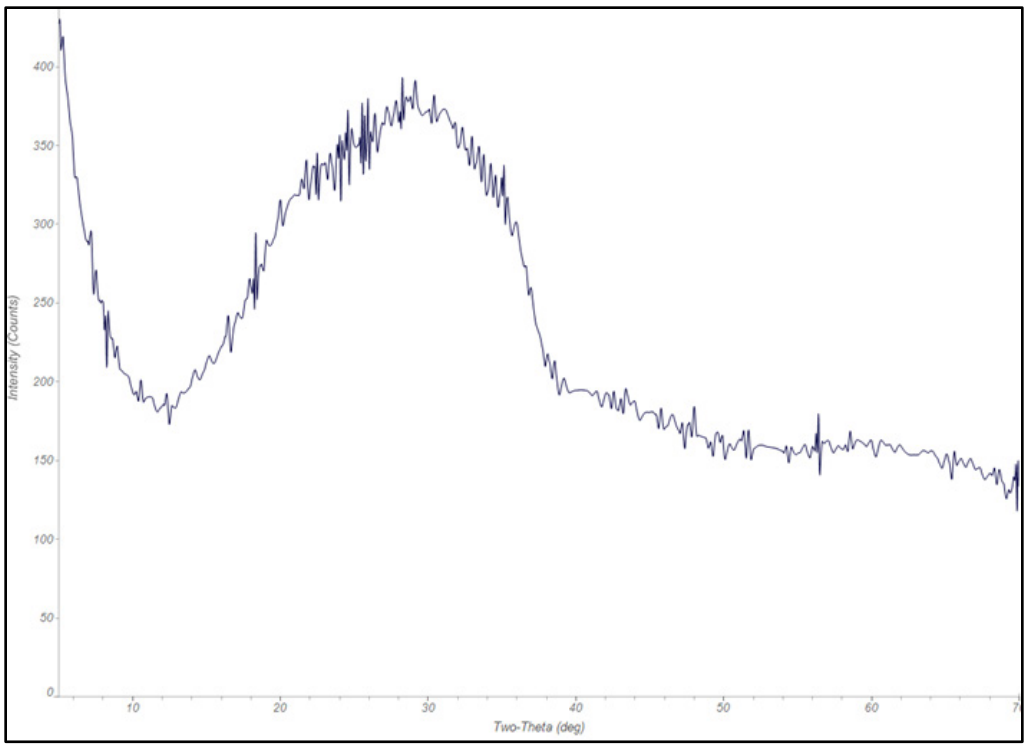

Figure A-16. X-ray diffraction pattern of NP2-23 cooled between 1150 ℃ and 650 ℃ at 2.0℃/min

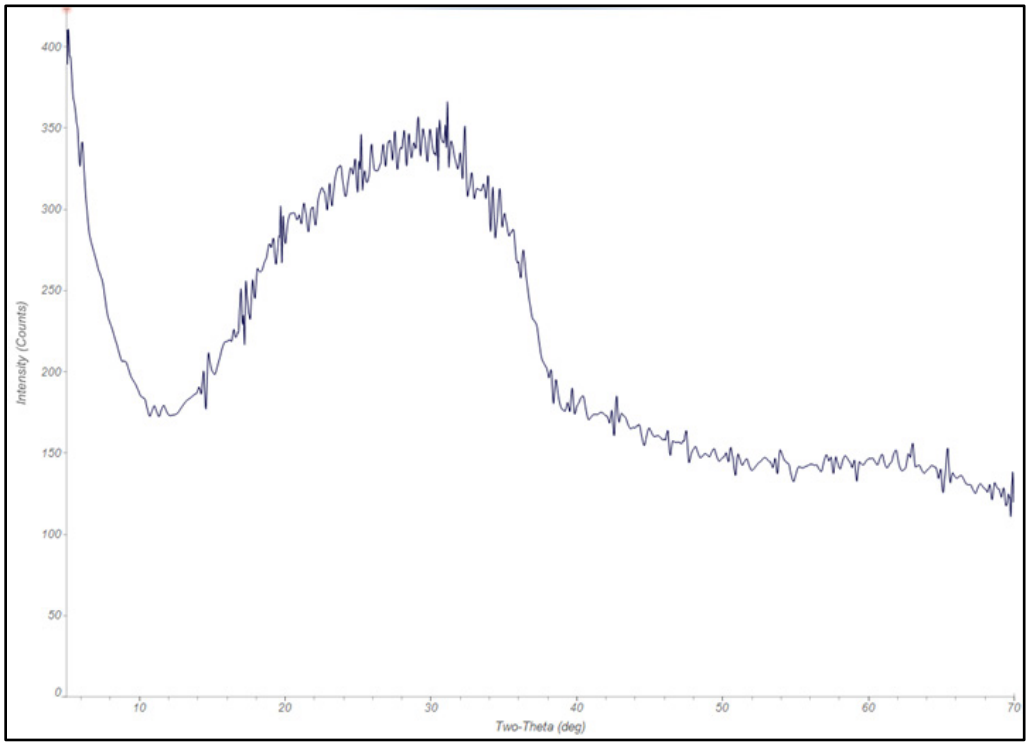

Figure A-17. X-ray diffraction pattern of NP2-23 cooled between 1150 ℃ and 550 ℃ at 2.0℃/min

XRD of Glass Composition, NP2-23 After 24 hr. Isothermal Heat Treatment:

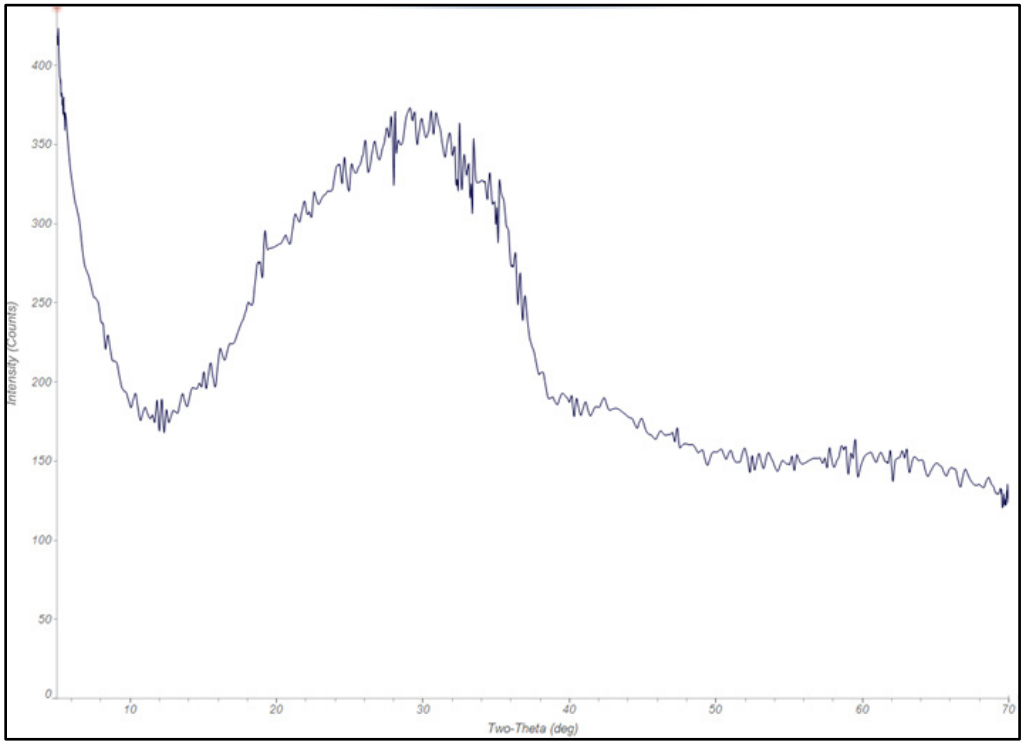

Figure A-18. X-ray diffraction pattern of NP2-23 held at 950 ℃ for 24 hr.

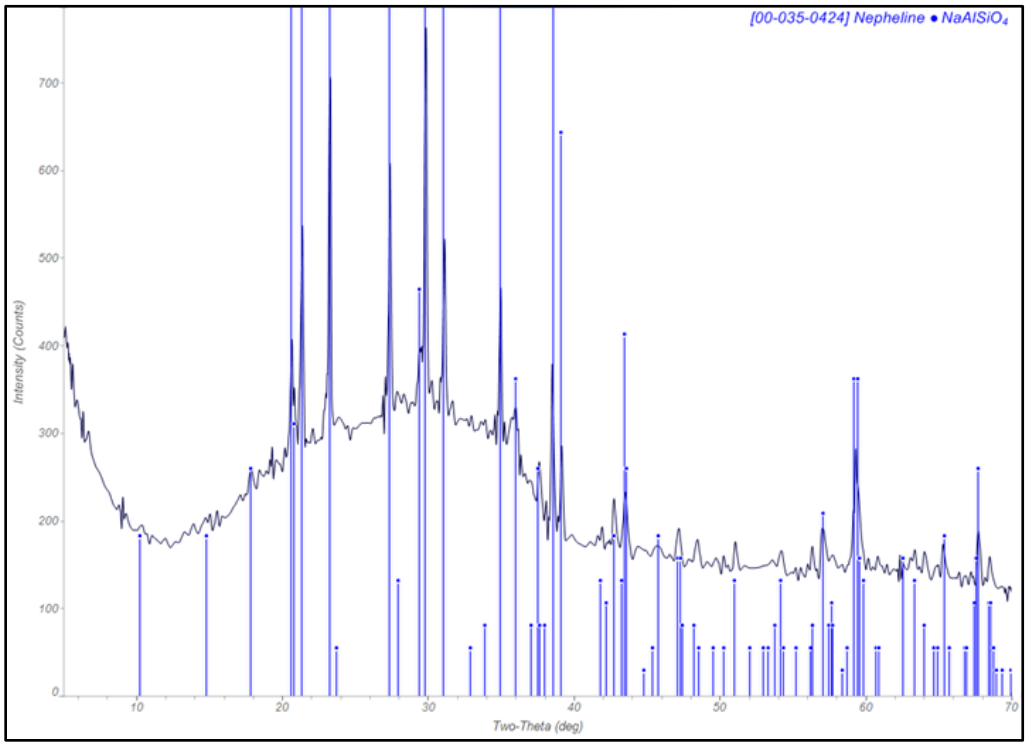

Figure A-19. X-ray diffraction pattern of NP2-23 held at 850 ℃ for 24 hr.

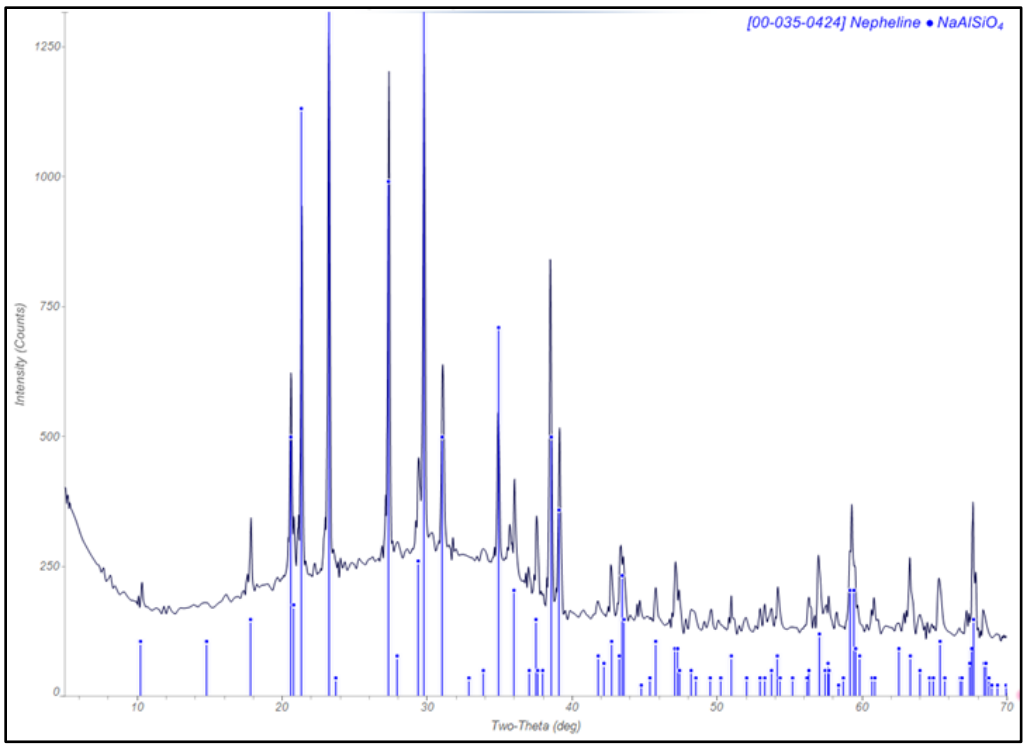

Figure A-20. X-ray diffraction pattern of NP2-23 held at 750 ℃ for 24 hr.

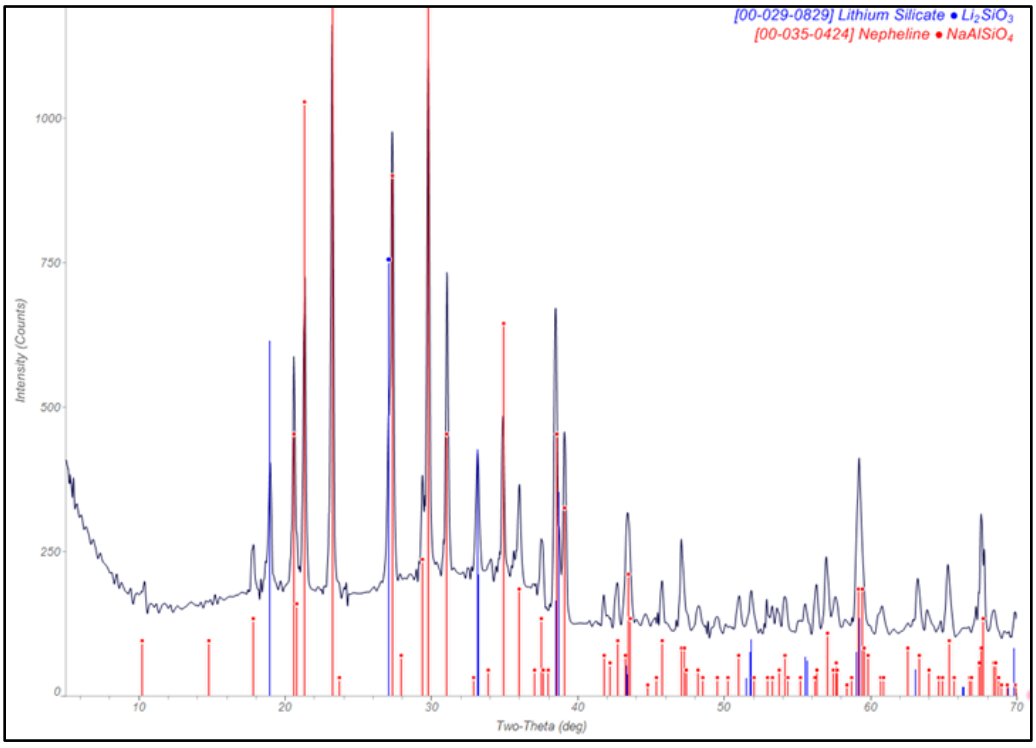

Figure A-21. X-ray diffraction pattern of NP2-23 held at 600 ℃ for 24 hr.

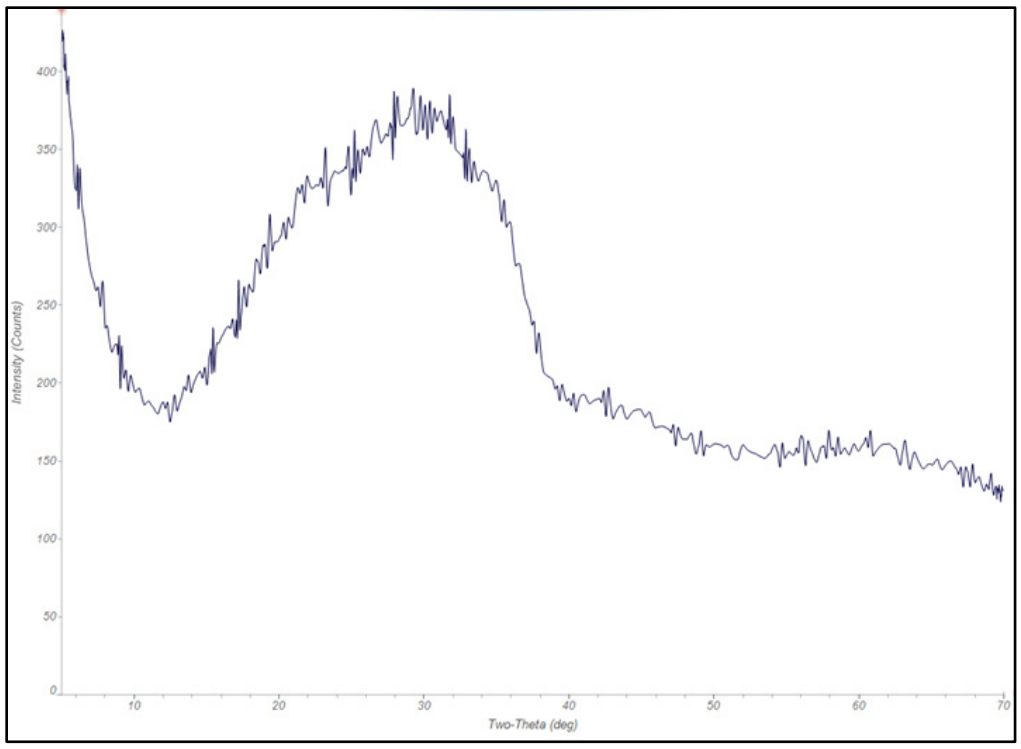

Figure A-22. X-ray diffraction pattern of NP2-23 held at 500 ℃ for 24 hr.

Distribution:

J. W. Amoroso, 999-W
T. B. Brown, 773-A
H. H. Burns, 773-41A
A. S. Choi, 999-W
J. H. Christian, 999-W
A. D. Cozzi, 999-W
C. L. Crawford, 773-42A
J. V. Crum, PNNL
S. D. Fink, 773-A
K. M. Fox, 999-W
J. C. Griffin, 773-A
E. K. Hansen, 999-W
C. C. Herman, 773-A
E. N. Hoffman, 999-W
J. E. Hyatt, 773-A
C. M. Jantzen, 773-A
F. C. Johnson, 999-W
D. S. Kim, PNNL
A. A. Kruger, DOE-ORP
J. C. Marra, 999-2W
J. Matyáš, PNNL
D. J. McCabe, 773-42A
D. L. McClane, 999-W
D. H. Miller, 999-W
D. K. Peeler, PNNL
F. M. Pennebaker, 773-42A
M. R. Poirier, 773-42A
M. J. Schweiger, PNNL
M. E. Stone, 999-W
J. D. Vienna, PNNL
A. L. Washington, 773-A
W. R. Wilmarth, 773-A
Records Administration (EDWS)